also be taken into consideration, such as possible anti-pruritic effects by the vehicle as an emollient. However, the use of emollients was allowed in both the tacrolimus monotherapy group and emollient group in maintenance treatment, thereby lessening this possibility.

In conclusion, topical tacrolimus is well tolerated (68/70 patients were able to complete the induction therapy) and significantly effective in controlling intractable pruritis during induction and maintenance therapy for patients with AD.

ACKNOWLEDGMENT

This work was supported by research grants from the Ministry of Health, Labour and Welfare, Japan. We thank Drs. Hiromichi Kai and Toyoaki Kato at the Department of Dermatology, University of Tokyo, for their outstanding help.

REFERENCES

1. Takeuchi M, Ueda H. Increase of adult atopic dermatitis (AD) in recent Japan. Environ Dermatol 2000;7:133-136.
2. Yamamoto S. Prevalence and exacerbation factors of atopic dermatitis. Skin Allergy Frontier 2003;1:85-90.
3. Ikoma A, Steinhoff M, Ständer S, Yosipovitch G, Schmelz M. The neurobiology of itch. Nat Rev Neurosci 2006;7:535-547.
4. Rossi R, Johansson O. Cutaneous innervation and the role of neuronal peptides in cutaneous inflammation: a minireview. Eur J Dermatol 1998;8:299-306.
5. Ständer S, Steinhoff M, Schmelz M, Weisshaar E, Metze D, Luger T. Neurophysiology of pruritus: cutaneous elicitation of itch. Arch Dermatol 2003;139:1463-1470.
6. Furue M, Terao H, Rikihisa W, Urabe K, Kinukawa N, Nose Y, et al. Clinical dose and adverse effects of topical steroids in daily management of atopic dermatitis. Br J Dermatol 2003;148:128-133.
7. Wahlgren CF. Itch and atopic dermatitis: clinical and experimental studies. Acta Derm Venereol Suppl (Stockh) 1991;165:1-53.
8. Boguniewicz M, Fiedler VC, Raimer S, Lawrence ID, Leung DY, Hanifin JM. A randomized, vehicle-controlled trial of tacrolimus ointment for treatment of atopic dermatitis in children. Pediatric Tacrolimus Study Group. J Allergy Clin Immunol 1998;102:637-644.
9. Severity scoring of atopic dermatitis: the SCORAD index. Consensus Report of the European Task Force on Atopic Dermatitis. Dermatology 1993;186:23-31.
10. Furue M, Terao H, Moroi Y, Koga T, Kubota Y, Nakayama J, et al. Dosage and adverse effects of topical tacrolimus and steroids in daily management of atopic dermatitis. J Dermatol 2004;31:277-283.
11. Fleischer AB Jr, Ling M, Eichenfield L, Satoi Y, Jaracz E, Rico MJ, et al. Tacrolimus ointment for the treatment of atopic dermatitis is not associated with an increase in cutaneous infections. J Am Acad Dermatol 2002;47:562-570.
12. Rivard J, Lim HW. Ultraviolet phototherapy for pruritus. Dermatol Ther 2005;18:344-354.
13. Chuang TY, Heinrich LA, Schultz MD, Reizner GT, Kumm RC, Cripps DJ. PUVA and skin cancer. A historical cohort study on 492 patients. J Am Acad Dermatol 1992;26:173-177.
14. Hon KL, Lam MC, Leung TF, Chow CM, Wong E, Leung AK. Assessing itch in children with atopic dermatitis treated with tacrolimus: objective versus subjective assessment. Adv Ther 2007;24:23-28.
15. Reitamo S, Rustin M, Ruzicka T, Cambazard F, Kalimo K, Friedmann PS, et al; European Tacrolimus Ointment Study Group. Efficacy and safety of tacrolimus ointment compared with that of hydrocortisone butyrate ointment in adult patients with atopic dermatitis. J Allergy Clin Immunol 2002;109:547-555.
16. Japanese FK-506 Ointment Study Group. Phase III study of FK-506 (Tacrolimus) ointment in patients with atopic dermatitis -Comparison study with 0.12% betamethasone valerate ointment for trunk and extremities lesions-. Nishinihon J Dermatol 1997;59:870-879. (article in Japanese)
17. Inagaki N, Shiraishi N, Igeta K, Itoh T, Chikumoto T, Nagao M, et al. Inhibition of scratching behavior associated with allergic dermatitis in mice by tacrolimus, but not by dexamethasone. Eur J Pharmacol 2006;546:189-196.
18. Inagaki N, Shiraishi N, Igeta K, Nagao M, Kim JF, Chikumoto T, et al. Depletion of substance P, a mechanism for inhibition of mouse scratching behavior by tacrolimus. Eur J Pharmacol 2010;626:283-289.
19. Inoue T, Katoh N, Kishimoto S. Prolonged topical application of tacrolimus inhibits immediate hypersensitivity reactions by reducing degranulation of mast cells. Acta Derm Venereol 2006;86:13-16.
20. Kido M, Takeuchi S, Esaki H, Hayashida S, Furue M. Scratching behavior does not necessarily correlate with epidermal nerve fiber sprouting or inflammatory cell infiltration. J Dermatol Sci 2010;58:130-135.
21. Takeuchi S, Yasukawa F, Furue M, Katz SI. Collared mice: a model to assess the effects of scratching. J Dermatol Sci 2010;57:44-50.

Genome-wide association study identifies eight new susceptibility loci for atopic dermatitis in the Japanese population

Tomomitsu Hirota[1], Atsushi Takahashi[2], Michiaki Kubo[3], Tatsuhiko Tsunoda[4], Kaori Tomita[5], Masafumi Sakashita[5], Takechiyo Yamada[5], Shigeharu Fujieda[5], Shota Tanaka[1,6], Satoru Doi[7], Akihiko Miyatake[8], Tadao Enomoto[9], Chiharu Nishiyama[10], Nobuhiro Nakano[10], Keiko Maeda[10], Ko Okumura[10], Hideoki Ogawa[10], Shigaku Ikeda[11], Emiko Noguchi[12,13], Tohru Sakamoto[14], Nobuyuki Hizawa[14], Koji Ebe[15], Hidehisa Saeki[16], Takashi Sasaki[17], Tamotsu Ebihara[17], Masayuki Amagai[17], Satoshi Takeuchi[18], Masutaka Furue[18], Yusuke Nakamura[19] & Mayumi Tamari[1]

Atopic dermatitis is a common inflammatory skin disease caused by interaction of genetic and environmental factors. On the basis of data from a genome-wide association study (GWAS) and a validation study comprising a total of 3,328 subjects with atopic dermatitis and 14,992 controls in the Japanese population, we report here 8 new susceptibility loci: *IL1RL1-IL18R1-IL18RAP* ($P_{combined} = 8.36 \times 10^{-18}$), the major histocompatibility complex (MHC) region ($P = 8.38 \times 10^{-20}$), *OR10A3-NLRP10* ($P = 1.54 \times 10^{-22}$), *GLB1* ($P = 2.77 \times 10^{-16}$), *CCDC80* ($P = 1.56 \times 10^{-19}$), *CARD11* ($P = 7.83 \times 10^{-9}$), *ZNF365* ($P = 5.85 \times 10^{-20}$) and *CYP24A1-PFDN4* ($P = 1.65 \times 10^{-8}$). We also replicated the associations of the *FLG*, *C11orf30*, *TMEM232-SLC25A46*, *TNFRSF6B-ZGPAT*, *OVOL1*, *ACTL9* and *KIF3A-IL13* loci that were previously reported in GWAS of European and Chinese individuals and a meta-analysis of GWAS for atopic dermatitis. These findings advance the understanding of the genetic basis of atopic dermatitis.

Atopic dermatitis is a chronic, relapsing skin disorder involving disturbed skin barrier functions, cutaneous inflammatory hypersensitivity and defects in antimicrobial immune defense with a strong genetic basis[1,2]. It is well established that common loss-of-function variants in *FLG* (encoding filaggrin) are a major predisposing factor for atopic dermatitis[3,4]. Association studies in populations of diverse ancestry, meta-analyses of studies and GWAS have shown that mutation in *FLG* is strongly associated with atopic dermatitis[4–7]. Apart from *FLG*, recent GWAS of European and Chinese populations for atopic dermatitis and a meta-analysis of GWAS have reported six susceptibility loci at a genome-wide level of significance—*C11orf30*, *TMEM232-SLC25A46*, *TNFRSF6B-ZGPAT*, *OVOL1*, *ACTL9* and *KIF3A-IL13*[5–7]. To gain a better understanding of the contribution of complex genetic effects to the pathogenesis of atopic dermatitis, it is important to identify additional susceptibility loci and validate the association of previously reported loci in different ancestry groups.

We performed a GWAS in the Japanese population with 1,472 individuals with atopic dermatitis (cases) and 7,971 controls using Illumina Human OmniExpress BeadChips (**Supplementary Table 1**). We subjected genotype data from a total of 606,164 SNPs to statistical analysis after principal-component analysis (PCA) and quality control filtering, and we generated a quantile-quantile plot using the Cochran-Armitage test (**Supplementary Fig. 1a–c**). The genomic inflation factor (λ_{GC}) was 1.03, indicating that there was a low possibility of false positive associations resulting from population stratification. The Manhattan plot showed that a total of 36 SNPs within 3 chromosomal regions at 2q12, 6p21.3 and 11p15.4 had associations that reached the genome-wide significance threshold of $P < 5 \times 10^{-8}$ (**Fig. 1**).

GWAS of European and Chinese populations and a meta-analysis of GWAS have reported seven susceptibly regions for atopic

[1]Laboratory for Respiratory Diseases, Center for Genomic Medicine, RIKEN, Yokohama, Japan. [2]Laboratory for Statistical Analysis, Center for Genomic Medicine, RIKEN, Minato-ku, Japan. [3]Laboratory for Genotyping Development, Center for Genomic Medicine, RIKEN, Yokohama, Japan. [4]Laboratory for Medical Informatics, Center for Genomic Medicine, RIKEN, Yokohama, Japan. [5]Department of Otorhinolaryngology, Fukui Medical University, Matsuoka, Japan. [6]Department of Otolaryngology–Head and Neck Surgery, University of Yamanashi, Faculty of Medicine, Chuo, Japan. [7]Osaka Prefectural Medical Center for Respiratory and Allergic Diseases, Habikino, Japan. [8]Miyatake Asthma Clinic, Osaka, Japan. [9]Nonprofit Organization (NPO) Japan Health Promotion Supporting Network, Wakayama, Japan. [10]Atopy Research Center, Juntendo University School of Medicine, Bunkyo-ku, Japan. [11]Department of Dermatology, Juntendo University School of Medicine, Bunkyo-ku, Japan. [12]Department of Medical Genetics, Majors of Medical Sciences, Graduate School of Comprehensive Human Sciences, University of Tsukuba, Tsukuba, Japan. [13]Japan Science and Technology Agency, Core Research for Evolutional Science and Technology (CREST), Saitama, Japan. [14]Division of Respiratory Medicine, Institute of Clinical Medicine, University of Tsukuba, Tsukuba, Japan. [15]Department of Dermatology, Takao Hospital, Kyoto, Japan. [16]Department of Dermatology, Jikei University School of Medicine, Minato-ku, Japan. [17]Department of Dermatology, Keio University School of Medicine, Shinjuku-ku, Japan. [18]Department of Dermatology, Graduate School of Medical Sciences, Kyushu University, Fukuoka, Japan. [19]Laboratory of Molecular Medicine, The Institute of Medical Science, The University of Tokyo, Minato-ku, Japan. Correspondence should be addressed to M.T. (tamari@src.riken.jp).

Received 27 April; accepted 11 September; published online 7 October 2012; doi:10.1038/ng.2438

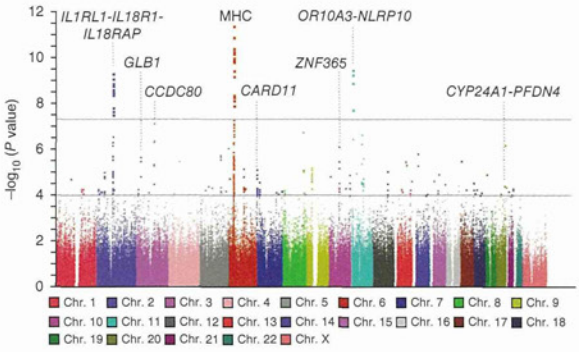

Figure 1 Manhattan plot showing the $-\log_{10} P$ values of 606,164 SNPs in the GWAS for 1,472 Japanese atopic dermatitis cases and 7,971 controls plotted against their respective positions on autosomes and the X chromosome. The red line shows the genome-wide significance threshold for this study ($P = 5 \times 10^{-8}$). The blue line shows the threshold ($P = 1 \times 10^{-4}$) for selecting SNPs for the validation study. Signals in the *IL1RL1-IL18R1-IL18RAP* (2q12), *GLB1* (3p21.33), *CCDC80* (3q13.2), MHC (6p21.3), *CARD11* (7p22), *ZNF365* (10q21.2), *OR10A3-NLRP10* (11p15.4) and *CYP24A1-PFDN4* (20q13) regions are indicated.

dermatitis[5–7]. We examined the previously reported regions in our GWAS and observed associations with atopic dermatitis for the SNPs in all of these regions (**Supplementary Fig. 2a–g** and **Supplementary Table 2**). Notably, the two regions identified in the previous GWAS of Chinese individuals had either the same SNP as the top signal in our study (20q13.3) or a SNP in strong linkage disequilibrium (LD) with the top SNP in the previous study (5q22.1); in contrast, for four of the five regions determined to be associated in Europeans, the top SNP in this study was in low LD with the previously reported best SNP.

To test for replication of the associations at the three loci suggested by the GWAS (2q12, 6p21.3 and 11p15.4) and to identify additional susceptibility loci for atopic dermatitis, we genotyped SNPs in a validation set consisting of a total of 1,856 individuals with atopic dermatitis and 7,021 controls (**Supplementary Table 1**). We first genotyped a total of ten tag SNPs ($r^2 < 0.80$) at the three loci and confirmed significant associations (**Supplementary Table 3**). We further investigated SNPs that showed P values of $<1 \times 10^{-4}$ in our GWAS and genotyped 87 tag SNPs ($r^2 < 0.80$) other than the previously reported loci and the three loci newly reported here. After Bonferroni correction with $P < 5.75 \times 10^{-4}$ (0.05/87), a total of 11 SNPs were found to be significantly associated with atopic dermatitis (**Supplementary Table 3**). We combined the data from the GWAS and

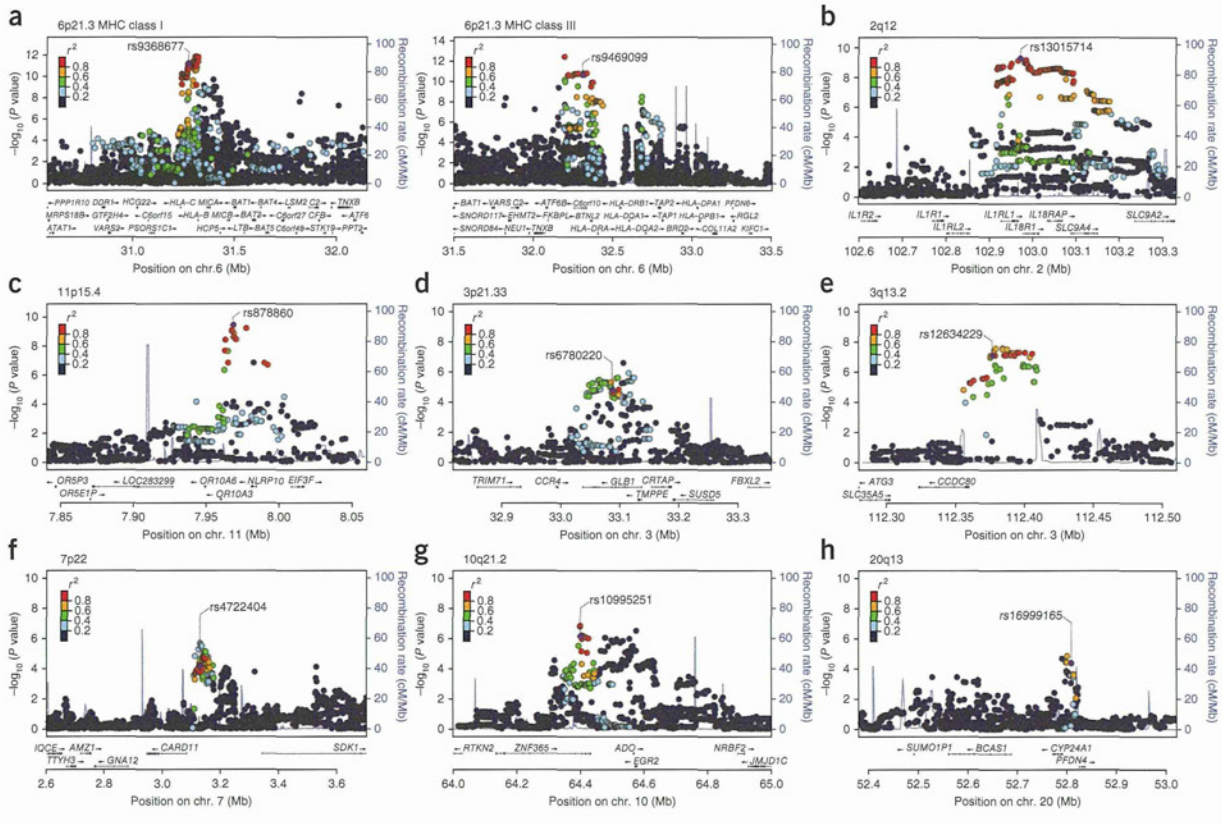

Figure 2 Regional plots of association results within eight newly identified susceptibility regions for atopic dermatitis. (**a**–**h**) Plots show the association results of both genotyped and imputed SNPs in the GWAS samples and the recombination rates within the susceptibility loci. For each plot, the $-\log_{10}$ P values (left y axis) of SNPs are shown according to their chromosomal positions (x axis). The genetic recombination rates are shown by the blue lines, and arrows indicate the locations of genes. The top genotyped SNP (labeled by rs number) is represented as a purple circle, and its LD (r^2) with the remaining SNPs is indicated by color. (**a**) MHC class I (left) and III (right) regions at 6p21.3. (**b**) 2q12. (**c**) 11p15.4. (**d**) 3p21.33. (**e**) 3q13.2. (**f**) 7p22. (**g**) 10q21.2. (**h**) 20q13.

Table 1 Summary of association results from the GWAS and validation study

SNP ID	Genes in or near regions of association	Chromosome (bp)	Allele (risk allele)	Stage	RAF		$P^{a,b}$	OR[b,c]	95% CI[b,c]	P_{het}[d]
					Case	Control				
rs13015714	*IL1RL1-IL18R1-IL18RAP*	2q12 (102971865)	T/G (G)	GWAS	0.473	0.412	5.17×10^{-10}	1.28	1.19–1.39	
				Validation	0.466	0.412	2.20×10^{-9}	1.25	1.16–1.34	
				Combined	0.470	0.412	8.36×10^{-18}	1.27	1.20–1.34	0.637
rs176095	*GPSM3* (MHC region)	6p21.3 (32158319)	T/C (T)	GWAS	0.860	0.811	3.86×10^{-10}	1.43	1.28–1.60	
				Validation	0.854	0.809	3.41×10^{-10}	1.38	1.25–1.53	
				Combined	0.856	0.810	8.38×10^{-20}	1.40	1.30–1.51	0.661
rs878860	*OR10A3-NLRP10*	11p15.4 (7968359)	A/G (G)	GWAS	0.603	0.540	3.47×10^{-10}	1.30	1.20–1.40	
				Validation	0.601	0.533	1.95×10^{-13}	1.32	1.23–1.42	
				Combined	0.602	0.537	1.54×10^{-22}	1.31	1.24–1.38	0.747
rs6780220	*GLB1*	3p21.33 (33087200)	T/G (G)	GWAS	0.582	0.539	1.55×10^{-5}	1.19	1.10–1.29	
				Validation	0.596	0.530	1.39×10^{-12}	1.31	1.21–1.41	
				Combined	0.590	0.535	2.77×10^{-16}	1.25	1.19–1.32	0.093
rs12634229	*CCDC80*	3q13.2 (112376308)	A/G (G)	GWAS	0.379	0.328	7.60×10^{-8}	1.25	1.15–1.36	
				Validation	0.391	0.326	8.18×10^{-14}	1.33	1.23–1.43	
				Combined	0.386	0.327	1.56×10^{-19}	1.29	1.22–1.37	0.303
rs4722404	*CARD11*	7p22 (3128789)	A/G (G)	GWAS	0.365	0.327	5.69×10^{-5}	1.18	1.09–1.28	
				Validation	0.362	0.325	2.67×10^{-5}	1.18	1.09–1.27	
				Combined	0.363	0.326	7.83×10^{-9}	1.18	1.12–1.25	0.911
rs10995251	*ZNF365*	10q21.2 (64398466)	T/C (C)	GWAS	0.568	0.518	7.73×10^{-7}	1.22	1.13–1.33	
				Validation	0.576	0.504	5.78×10^{-15}	1.34	1.24–1.44	
				Combined	0.572	0.511	5.85×10^{-20}	1.28	1.22–1.36	0.107
rs16999165	*CYP24A1-PFDN4*	20q13 (52807221)	T/C (T)	GWAS	0.729	0.691	3.87×10^{-5}	1.21	1.10–1.32	
				Validation	0.726	0.694	1.47×10^{-4}	1.17	1.08–1.27	
				Combined	0.728	0.692	1.65×10^{-8}	1.19	1.12–1.26	0.618

RAF, risk allele frequency; OR, odds ratio; CI, confidence interval.
[a]*P* values of the Cochran-Armitage trend test for each stage. [b]Results of combined analyses were calculated by the Mantel-Haenszel method. [c]Odds ratios and confidence intervals were calculated using the non-risk allele as a reference. [d]Results from the Breslow-Day test.

the validation set by the Mantel-Haenszel method, and a total of eight loci were found to be associated with atopic dermatitis at genome-wide significance (**Figs. 1** and **2** and **Table 1**). The Breslow-Day test showed an absence of significant heterogeneity ($P > 0.05$) (**Table 1**). We further assessed interactions among the eight newly discovered loci using the GWAS and validation data. We also conducted epistasis analysis, including the seven previously published loci, using the GWAS data. However, there was no evidence of an epistatic effect on susceptibility to atopic dermatitis with any combination of the 15 loci (**Supplementary Table 4**).

We obtained association results for >7 million imputed SNPs. In this study, a subset of genotype data for controls in the validation study was obtained from the GWAS data, but DNA samples were not available (**Supplementary Table 1**). Other cases and controls in the validation study were directly genotyped for SNPs at each locus. Thus, we focused on the directly genotyped SNPs in our GWAS and conducted a validation study. By imputation, we found that a total of 79 SNPs in 30 chromosomal regions were associated with atopic dermatitis at $5 \times 10^{-8} < P < 1 \times 10^{-4}$ (**Supplementary Table 5**). Further studies are needed to characterize the 30 regions suggested by imputation to associate with atopic dermatitis.

We next conducted conditional logistic regression analysis of the eight newly discovered loci using the GWAS data (**Supplementary Fig. 3**). This analysis indicated that there were two independent association signals in the MHC class I and III regions, one between *HLA-C* and *HLA-B* (rs9368677) and the other within *C6orf10* (rs9469099) (**Fig. 2a** and **Supplementary Fig. 3a**). In the *ZNF365* region, we observed independent signals at rs10995251, rs1444418 and rs10822056 (**Supplementary Fig. 3b**); however, the associations at rs1444418 and rs10822056 did not reach genome-wide significance when we combined the data from the GWAS and validation study ($P = 1.73 \times 10^{-7}$ and 1.15×10^{-4}, respectively). There were no independent signals in the other six associated regions (**Supplementary Fig. 3c–h**).

The associated region at 2q12 contains genes encoding the receptors of interleukin (IL)-1 family cytokines: *IL1RL1*, *IL18R1* and *IL18RAP* (**Fig. 2b** and **Table 1**). IL-1 family members are abundantly expressed in the skin[8]. IL1RL1, a component of the IL-33 receptor, is expressed by T helper type 2 (T_H2) cells and mast cells[9]. It has been reported that IL-33 is secreted in the damaged tissues of atopic dermatitis and promotes T_H2-type immune responses and the pathogenesis of atopic dermatitis[9]. The IL-1 receptor cluster region at 2q12 and the *IL33* region at 9p24.1 have also been identified as susceptibility loci by recent GWAS for bronchial asthma[10,11].

We found the most significant association with atopic dermatitis at rs176095 in the MHC class III region when we combined the data from the GWAS and validation study (**Fig. 2a** and **Table 1**). To our knowledge, this is the first finding of an association of atopic dermatitis with the MHC region at a genome-wide significance level. The MHC region is associated with a number of autoimmune diseases[12], and the involvement of autoimmunity in chronic inflammation in individuals with atopic dermatitis has been suggested[1]. Immunoglobulin E (IgE) antibodies against keratinocytes and endothelial cells are observed in serum specimens from subjects with severe atopic dermatitis[13].

The region of association at 11p15.4 includes two genes, *OR10A3* and *NLRP10* (**Fig. 2c** and **Table 1**). *OR10A3* is an olfactory receptor family gene, and *NLRP10* encodes a protein that belongs to the NALP protein family but lacks the leucine-rich repeat region. Individuals with atopic dermatitis are particularly susceptible to a number of microbial organisms, and pruritus is a major symptom of atopic dermatitis[1,2]. The itch-scratch cycle can lead to damage of the epidermal keratinocytes[1]. NLRP proteins are involved in sensing both microbial and danger signals[14], and NLRP10 has an anti-inflammatory

role through negative regulatory effects on caspase-1–dependent IL-1β secretion and apoptosis-associated speck-like protein containing a caspase recruitment domain (ASC)-mediated nuclear factor (NF)-κB activation[15].

The chromosome 3p21.33 region contains four genes, and the most significantly associated SNP, rs6780220, was located within *GLB1*, which encodes β-galactosidase-1 (**Fig. 2d** and **Table 1**). Notably, the associated region is located adjacent to the *CCR4* gene, which encodes a T_H2-associated chemokine receptor for CCL22 and CCL17 (also known as TARC). Keratinocyte-derived TSLP induces dendritic cells to produce TARC, and CCR4 mediates skin-specific recruitment of T cells during inflammation[1,16].

The associated region at 3q13.2 contains *CCDC80* (**Fig. 2e** and **Table 1**), which encodes a protein involved in the induction of C/EBPα and peroxisome proliferator-activated receptor γ (PPARγ)[17]. C/EBPα and C/EBPβ are coexpressed in basal keratinocytes and are upregulated when keratinocytes exit the basal layer and undergo terminal differentiation[18]. PPARγ acts as a negative regulator in immune cells, and a PPARγ agonist markedly suppresses both expression of thymic stromal lymphopoietin (TSLP) in the skin and maturation and migration of dendritic cells in a mouse model of atopic dermatitis[19].

The associated region at 7p22 contains *CARD11* (**Fig. 2f** and **Table 1**), which encodes CARMA1, an essential scaffold protein for lymphocyte activation via T-cell receptor (TCR) and B-cell receptor (BCR) signaling[20]. CARMA1 has an essential role in T-cell differentiation as well as a critical role in the regulation of the JunB and GATA3 transcription factors and the subsequent production of T_H2 cell–specific cytokines[21]. Mice that are homozygous for the mutation affecting Carma-1 show gradual development of atopic dermatitis with very high levels of serum IgE[22].

The region of association at 10q21.2 contains three genes, and the most significantly associated SNP, rs10995251, was located within *ZNF365* (**Fig. 2g** and **Table 1**). The region was reported to show suggestive association with atopic dermatitis ($P = 1.05 \times 10^{-7}$) by the previous GWAS of Chinese individuals[6], in which the association reached the genome-wide significance level. Notably, the region contains *EGR2*, which encodes a T-cell anergy-associated transcription factor that activates the expression of genes involved in the negative regulation of T-cell proliferation and inflammation[23].

The associated region at 20q13 includes *CYP24A1* and *PFDN4* (**Fig. 2h** and **Table 1**). *PFDN4* encodes a subunit of prefoldin, which is a molecular chaperone complex. *CYP24A1* encodes a mitochondrial cytochrome P450 superfamily enzyme. The protein initiates the degradation of 1,5-dihydroxyvitamin D3, the active form of vitamin D_3, by hydroxylation of the side chain[24]. Vitamin D is a modulator of innate and adaptive immune system functions[24], and an association between vitamin D deficiency and the severity of atopic dermatitis has been reported[25].

In this study, we identified variants at the *IL1RL1* and human leukocyte antigen (HLA) loci that associated with atopic dermatitis and replicated the associations at the *KIF3A-IL13* and *C11orf30* regions. The *C11orf30* region contains *LRRC32*, a gene previously reported to be specifically expressed in activated human naturally occurring regulatory T cells (nTreg)[26]. Atopic march is the natural history of atopic manifestations, and the clinical signs of atopic dermatitis generally predate the development of asthma and allergic rhinitis[27]. Recent GWAS have identified associations of the *IL1RL1*, HLA, *IL13* and *C11orf30* regions with bronchial asthma[10,11,28,29] and association of the *C11orf30* region with allergic rhinitis[30]. These findings suggest that atopic dermatitis and asthma or allergic rhinitis have overlapping susceptibility regions and that these regions contain common genetic factors for many allergic diseases. We stratified the cases by comorbidity of asthma and conducted an association study of asthma in the Japanese atopic dermatitis population for a total of 15 SNPs in the 7 previously reported and 8 newly identified regions. Notably, the most significant association was observed in the *IL1RL1* region ($P = 7.04 \times 10^{-9}$) (**Supplementary Table 6**).

In conclusion, we identified eight new susceptibility loci for atopic dermatitis at genome-wide significance, and we replicated the seven previously reported loci associated with atopic dermatitis in the Japanese population. Candidate genes at these loci suggest roles for epidermal barrier functions (*FLG* and *OVOL1*), adaptive immunity (*TNFRSF6B*, *IL13* and *CARD11*), IL-1 family signaling (*IL1RL1*, *IL18R1* and *IL18RAP*), negative regulation of apoptosis and the inflammatory response (*NALP10*), regulatory T cells (*LRRC32* and *EGR2*) and the vitamin D pathway (*CYP24A1*) in the pathogenesis of atopic dermatitis. Further studies are needed to better understand the genetic etiology and pathophysiology of atopic dermatitis.

URLs. The Leading Project for Personalized Medicine, http://biobankjp.org/; Haploview v4.2, http://www.broadinstitute.org/haploview/haploview; R statistical environment version 2.14.1, http://www.r-project.org/; minimac, http://genome.sph.umich.edu/wiki/Minimac; PLINK statistical software v1.07, http://pngu.mgh.harvard.edu/~purcell/plink/; LocusZoom, http://csg.sph.umich.edu/locuszoom/.

METHODS

Methods and any associated references are available in the online version of the paper.

Note: Supplementary information is available in the online version of the paper.

ACKNOWLEDGMENTS

We thank all the individuals who participated in the study and also thank the collaborating physicians for helping with sample collection. We are grateful to the members of BioBank Japan and the Rotary Club of Osaka-Midosuji District 2660 Rotary International in Japan for supporting our study. We thank M.T. Shimizu, H. Sekiguchi, A.I. Jodo, N. Kawaraichi and the technical staff of the Center for Genomic Medicine for providing technical assistance and K. Barrymore for proofreading this manuscript. This work was conducted as part of the BioBank Japan Project, which is supported by the Ministry of Education, Culture, Sports, Science and Technology, Japan. This work was also partly supported by grants from the Ministry of Health, Labour and Welfare, Japan.

AUTHOR CONTRIBUTIONS

T.H. and M.T. designed the study and drafted the manuscript. A.T. and T.T. analyzed the GWAS data. T.H., K.T., S. Tanaka and M.K. performed the genotyping for the GWAS. M.S., T.Y., S.F., S.D., A.M., T. Enomoto, C.N., N.N., K.M., S.I., K.O., H.O., E.N., T. Sakamoto, N.H., K.E., H.S., T. Sasaki, T. Ebihara, M.A., S. Takeuchi and M.F. recruited subjects and participated in the diagnostic evaluations. M.T. wrote the manuscript. M.K. and Y.N. contributed to the overall GWAS study design.

COMPETING FINANCIAL INTERESTS

The authors declare no competing financial interests.

Published online at http://www.nature.com/doifinder/10.1038/ng.2438.
Reprints and permissions information is available online at http://www.nature.com/reprints/index.html.

1. Bieber, T. Mechanisms of disease: atopic dermatitis. *N. Engl. J. Med.* **358**, 1483–1494 (2008).
2. Boguniewicz, M. & Leung, D.Y. Recent insights into atopic dermatitis and implications for management of infectious complications. *J. Allergy Clin. Immunol.* **125**, 4–13 (2010).
3. Palmer, C.N. *et al.* Common loss-of-function variants of the epidermal barrier protein filaggrin are a major predisposing factor for atopic dermatitis. *Nat. Genet.* **38**, 441–446 (2006).

4. Irvine, A.D., McLean, W.H. & Leung, D.Y. Filaggrin mutations associated with skin and allergic diseases. *N. Engl. J. Med.* **365**, 1315–1327 (2011).
5. Esparza-Gordillo, J. *et al.* A common variant on chromosome 11q13 is associated with atopic dermatitis. *Nat. Genet.* **41**, 596–601 (2009).
6. Sun, L.D. *et al.* Genome-wide association study identifies two new susceptibility loci for atopic dermatitis in the Chinese Han population. *Nat. Genet.* **43**, 690–694 (2011).
7. Paternoster, L. *et al.* Meta-analysis of genome-wide association studies identifies three new risk loci for atopic dermatitis. *Nat. Genet.* **44**, 187–192 (2012).
8. Johnston, A. *et al.* IL-1F5, -F6, -F8, and -F9: a novel IL-1 family signaling system that is active in psoriasis and promotes keratinocyte antimicrobial peptide expression. *J. Immunol.* **186**, 2613–2622 (2011).
9. Liew, F.Y., Pitman, N.I. & McInnes, I.B. Disease-associated functions of IL-33: the new kid in the IL-1 family. *Nat. Rev. Immunol.* **10**, 103–110 (2010).
10. Moffatt, M.F. *et al.* A large-scale, consortium-based genomewide association study of asthma. *N. Engl. J. Med.* **363**, 1211–1221 (2010).
11. Torgerson, D.G. *et al.* Meta-analysis of genome-wide association studies of asthma in ethnically diverse North American populations. *Nat. Genet.* **43**, 887–892 (2011).
12. Horton, R. *et al.* Gene map of the extended human MHC. *Nat. Rev. Genet.* **5**, 889–899 (2004).
13. Altrichter, S. *et al.* Serum IgE autoantibodies target keratinocytes in patients with atopic dermatitis. *J. Invest. Dermatol.* **128**, 2232–2239 (2008).
14. Magalhaes, J.G. *et al.* What is new with Nods? *Curr. Opin. Immunol.* **23**, 29–34 (2011).
15. Imamura, R. *et al.* Anti-inflammatory activity of PYNOD and its mechanism in humans and mice. *J. Immunol.* **184**, 5874–5884 (2010).
16. Vestergaard, C. *et al.* A Th2 chemokine, TARC, produced by keratinocytes may recruit CLA$^+$CCR4$^+$ lymphocytes into lesional atopic dermatitis skin. *J. Invest. Dermatol.* **115**, 640–646 (2000).
17. Tremblay, F. *et al.* Bidirectional modulation of adipogenesis by the secreted protein Ccdc80/DRO1/URB. *J. Biol. Chem.* **284**, 8136–8147 (2009).
18. Lopez, R.G. *et al.* C/EBPα and β couple interfollicular keratinocyte proliferation arrest to commitment and terminal differentiation. *Nat. Cell Biol.* **11**, 1181–1190 (2009).
19. Jung, K. *et al.* Peroxisome proliferator-activated receptor γ–mediated suppression of dendritic cell function prevents the onset of atopic dermatitis in NC/Tnd mice. *J. Allergy Clin. Immunol.* **127**, 420–429 (2011).
20. Hara, H. *et al.* Cell type–specific regulation of ITAM-mediated NF-κB activation by the adaptors, CARMA1 and CARD9. *J. Immunol.* **181**, 918–930 (2008).
21. Blonska, M. *et al.* CARMA1 controls Th2 cell–specific cytokine expression through regulating JunB and GATA3 transcription factors. *J. Immunol.* **188**, 3160–3168 (2012).
22. Jun, J.E. *et al.* Identifying the MAGUK protein Carma-1 as a central regulator of humoral immune responses and atopy by genome-wide mouse mutagenesis. *Immunity* **18**, 751–762 (2003).
23. Safford, M. *et al.* Egr-2 and Egr-3 are negative regulators of T cell activation. *Nat. Immunol.* **6**, 472–480 (2005).
24. Hart, P.H., Gorman, S. & Finlay-Jones, J.J. Modulation of the immune system by UV radiation: more than just the effects of vitamin D? *Nat. Rev. Immunol.* **11**, 584–596 (2011).
25. Peroni, D.G. *et al.* Correlation between serum 25–hydroxyvitamin D levels and severity of atopic dermatitis in children. *Br. J. Dermatol.* **164**, 1078–1082 (2011).
26. Wang, R. *et al.* Expression of GARP selectively identifies activated human FOXP3$^+$ regulatory T cells. *Proc. Natl. Acad. Sci. USA* **106**, 13439–13444 (2009).
27. Spergel, J.M. & Paller, A.S. Atopic dermatitis and the atopic march. *J. Allergy Clin. Immunol.* **112**, S118–S127 (2003).
28. Hirota, T. *et al.* Genome-wide association study identifies three new susceptibility loci for adult asthma in the Japanese population. *Nat. Genet.* **43**, 893–896 (2011).
29. Ferreira, M.A. *et al.* Identification of *IL6R* and chromosome 11q13.5 as risk loci for asthma. *Lancet* **378**, 1006–1014 (2011).
30. Ramasamy, A. *et al.* A genome-wide meta-analysis of genetic variants associated with allergic rhinitis and grass sensitization and their interaction with birth order. *J. Allergy Clin. Immunol.* **128**, 996–1005 (2011).

ONLINE METHODS

Study subjects. Characteristics of each case-control group are shown in **Supplementary Table 1**. All subjects with atopic dermatitis were diagnosed by physicians according to the criteria of Hanifin and Rajka[31]. All individuals were Japanese and gave written informed consent to participate in the study. This research project was approved by the ethical committees at the Institute of Medical Science, the University of Tokyo and the RIKEN Yokohama Institute.

BioBank Japan cases. The BioBank Japan project has been running since 2003, aiming at the collection of basic information for application to personalized medicine[32]. We selected case samples from the subjects who participated in the BioBank Japan, and a total of 1,472 cases for the GWAS and 940 cases for the validation study were recruited from several medical institutes, including the Fukujuji Hospital, Iizuka Hospital, Juntendo University, Hospital Iwate Medical University School of Medicine, National Hospital Organization Osaka National Hospital, Nihon University, Nippon Medical School, Shiga University of Medical Science, Cancer Institute Hospital of the Japanese Foundation for Cancer Research, Tokushukai Hospital and Tokyo Metropolitan Geriatric Hospital in Japan.

RIKEN cases. For the validation study, a total of 916 cases were recruited from the Takao Hospital, Kyushu University Hospital, University of Tokyo Hospital, Keio University Hospital, University of Tsukuba Hospital and several other hospitals.

BioBank controls. We used genome-wide screening data from subjects in the BioBank Japan project for the controls. Individuals with bronchial asthma and atopic dermatitis were excluded from the controls. Controls for the GWAS consisted of 6,042 cases in BioBank Japan with 1 of 5 diseases (cerebral aneurysm, esophageal cancer, endometrial cancer, chronic obstructive pulmonary disease and glaucoma), 1,023 healthy volunteers from members of the Rotary Club of Osaka-Midosuji District 2660 Rotary International in Japan[33] and 906 healthy subjects from the PharmaSNP Consortium.

A total of 5,547 cases registered in BioBank Japan with 1 of 4 diseases (epilepsy, urolithiasis, nephrotic syndrome and Graves' disease) were recruited for the validation study.

RIKEN controls. A total of 1,474 healthy volunteers were recruited from several medical institutes in Japan, including the Japanese Red Cross Wakayama Medical Center, Fukui University and Tsukuba University. Individuals with bronchial asthma and atopic dermatitis were excluded from the control group.

Genotyping and quality control. For the GWAS, we genotyped 1,491 cases and 7,983 controls using the Illumina Human OmniExpress BeadChip. We excluded a total of 19 cases and 12 controls because allele sharing analysis revealed that they were closely related, paired samples. We performed PCA of genotype data from the subjects along with data from European (CEU), African (YRI) and east Asian (Japanese (JPT) and Han Chinese (CHB) individuals obtained from the Phase 2 HapMap database by using smartpca[34]. The PCA plot indicated that cases and controls were genetically matched, with minimal evidence of population stratification (**Supplementary Fig. 1a,b**). We excluded samples with a call rate for autosomal SNPs of <0.98. We also excluded SNPs with minor allele frequencies of less than 0.01 from both cases and controls. SNPs having call rates of ≥99% in both cases and controls were used for the association study. We conducted exact Hardy-Weinberg equilibrium analysis, and SNPs with P values less than the cutoff value for the Hardy-Weinberg equilibrium test ($P < 1 \times 10^{-6}$ in controls) were excluded from the analysis.

In the validation study, we genotyped SNPs using the TaqMan assay (Life Technologies) or the multiplex PCR–based Invader assay (Third Wave Technologies). The genotype concordance rates for the eight SNPs in **Table 1** between samples genotyped using the Illumina Human OmniExpress BeadChip and those same samples genotyped with the TaqMan assay or multiplex PCR–based Invader assay were 1.000 and 1.000, respectively.

Statistical analysis. In the GWAS and validation study, the statistical significance of the association with each SNP was assessed using a 1-degree-of-freedom Cochran-Armitage trend test. We assessed association of SNPs on chromosome X by a meta-analysis with the Mantel-Haenszel method for two 2 × 2 allele frequency tables within male and female subjects. Odds ratios and confidence intervals were calculated from a 2 × 2 allele frequency table. We combined data from the GWAS and validation study by the Mantel-Haenszel method. Heterogeneity across the studies was examined using the Breslow-Day test[35]. Regional association plots were generated using LocusZoom[36].

Imputation. Imputation provides a high-resolution view of an associated region. Genotype imputation within the GWAS was performed using minimac. Association tests were performed with mach2dat using the fractional dosages output[37,38]. We used individuals from the 1000 Genomes Project (phased JPN, CHB and Han Chinese South (CHS) data, June 2011) as reference populations[39]. SNPs with a minor allele frequency of <5% and low quality of imputation ($r^2 < 0.7$) were excluded.

31. Hanifin, J.M. & Rajka, R.G. Diagnostic features of atopic dermatitis. *Acta Derm. (Stockholm)* **92** (suppl. 92), 44–47 (1980).
32. Nakamura, Y. The BioBank Japan Project. *Clin. Adv. Hematol. Oncol.* **5**, 696–697 (2007).
33. Takata, R. *et al.* Genome-wide association study identifies five new susceptibility loci for prostate cancer in the Japanese population. *Nat. Genet.* **42**, 751–754 (2010).
34. Price, A.L. *et al.* Principal components analysis corrects for stratification in genome-wide association studies. *Nat. Genet.* **38**, 904–909 (2006).
35. Breslow, N.E. & Day, N.E. Statistical methods in cancer research. Volume II—the design and analysis of cohort studies. *IARC Sci. Publ.* 1–406 (1987).
36. Pruim, R.J. *et al.* LocusZoom: regional visualization of genome-wide association scan results. *Bioinformatics* **26**, 2336–2337 (2010).
37. Li, Y. *et al.* MaCH: using sequence and genotype data to estimate haplotypes and unobserved genotypes. *Genet. Epidemiol.* **34**, 816–834 (2010).
38. Li, Y. *et al.* Genotype imputation. *Annu. Rev. Genomics Hum. Genet.* **10**, 387–406 (2009).
39. 1000 Genomes Project Consortium. A map of human genome variation from population-scale sequencing. *Nature* **467**, 1061–1073 (2010).

See related commentary on pg 7

ORIGINAL ARTICLE

Identification of Ketoconazole as an AhR-Nrf2 Activator in Cultured Human Keratinocytes: The Basis of Its Anti-Inflammatory Effect

Gaku Tsuji[1,3], Masakazu Takahara[1,3], Hiroshi Uchi[1,2], Tetsuo Matsuda[1], Takahito Chiba[1,2], Satoshi Takeuchi[1], Fumiko Yasukawa[1,2], Yoichi Moroi[1] and Masutaka Furue[1,2]

Ketoconazole (KCZ) has been shown to exhibit anti-inflammatory effects in addition to its inhibitory effects against fungi; however, the underlying molecular mechanism remains poorly understood. Aryl hydrocarbon receptor (AhR), a receptor that is activated by polycyclic aromatic hydrocarbons (PAHs) and halogenated aromatic hydrocarbons such as dioxin, is a sensor of the redox system against oxidative stress and regulates nuclear factor-erythroid 2-related factor-2 (Nrf2), a master switch of the redox machinery. To clarify whether KCZ modulates AhR-Nrf2 function leading to redox system activation, cultured human keratinocytes were treated with KCZ. Confocal microscopic analysis revealed that KCZ induced AhR nuclear translocation, resulting in the upregulation of CYP1A1 mRNA and protein expression. Furthermore, KCZ actively switched on Nrf2 nuclear translocation and quinone oxidoreductase 1 expression. Tumor necrosis factor-α- and benzo(a)pyrene (BaP)-induced reactive oxidative species (ROS) and IL-8 production were effectively inhibited by KCZ. Knockdown of either AhR or Nrf2 abolished the inhibitory capacity of KCZ on ROS and IL-8 production. In addition, KCZ-induced Nrf2 activation was canceled by AhR knockdown. Moreover, KCZ inhibited BaP-induced 8-hydroxydeoxyguanosine and IL-8 production. In conclusion, the engagement of AhR by KCZ exhibits the cytoprotective effect mediated by the Nrf2 redox system, which potently downregulates either cytokine-induced (AhR-independent) or PAH-induced (AhR-dependent) oxidative stress.

Journal of Investigative Dermatology (2012) **132,** 59-68; doi:10.1038/jid.2011.194; published online 14 July 2011

INTRODUCTION

Ketoconazole (KCZ) is an azole antifungal agent. KCZ may be particularly effective against inflammatory skin diseases, including psoriasis (Farr *et al.*, 1985), acne (De Pedrini *et al.*, 1988), and atopic dermatitis (Bäck *et al.*, 1995). The mechanism by which KCZ inhibits skin inflammation has largely depended on its suppression of *Malassezia* spp, which contributes to the aggravation of seborrheric dermatitis (Gupta *et al.*, 2004) and atopic dermatitis (Darabi *et al.*, 2009). However, KCZ also exerts a direct anti-inflammatory effect (Kanda and Watanabe, 2006; Nakashima *et al.*, 2007), the mechanism of which has remained largely unknown.

Several studies of oral KCZ-induced hepatic dysfunction have revealed that KCZ induces aryl hydrocarbon receptor (AhR) signaling-mediated genes in human hepatocytes (Casley *et al.*, 2007; Korashy *et al.*, 2007). AhR is activated by polycyclic aromatic hydrocarbons (PAHs) and halogenated aromatic hydrocarbons such as dioxin. Specifically, AhR signaling occurs as follows (Ma and Lu, 2003): (1) the ligand interacts with AhR in the cytoplasm; (2) the ligand–AhR complex translocates from the cytoplasm into the nucleus; (3) the ligand–AhR complex forms a heterodimer ligand/AhR/AhR nuclear translocator in the nucleus; and (4) the ligand/AhR/AhR nuclear translocator complex binds to xenobiotic response elements and activates the transcription of some members of the cytochrome P450 enzyme family such as CYP1A1, which metabolizes and activates the ligand. Previous studies, including our report, have shown that AhR signaling in normal human epidermal keratinocytes (NHEKs) functions as a metabolizing system for PAHs such as benzo(a)pyrene (BaP; Khan *et al.*, 1992; Tsuji *et al.*, 2011).

Furthermore, AhR signaling has a cross-talk with other transcription factors (Köhle and Bock, 2007; Haarmann-Stemmann *et al.*, 2009). In the present study, we focused on

[1]*Department of Dermatology, Graduate School of Medical Sciences, Kyushu University, Fukuoka, Japan and* [2]*Research and Clinical Center for Yusho and Dioxin, Kyushu University Hospital, Fukuoka, Japan*

[3]*These authors contributed equally to this work.*

Correspondence: Gaku Tsuji, Department of Dermatology, Graduate School of Medical Sciences, Kyushu University, 3-1-1 Maidashi, Higashi-ku, Fukuoka 812-8582, Japan. E-mail: gakku@dermatol.med.kyushu-u.ac.jp

Abbreviations: 8-OHdG, 8-hydroxydeoxyguanosine; AhR, aryl hydrocarbon receptor; AhRR, aryl hydrocarbon receptor repressor; ARE, antioxidant response elements; BaP, benzo(a)pyrene; KCZ, ketoconazole; NHDF, normal human dermal fibroblast; NHEK, normal human epidermal keratinocyte; Nqo1, NAD(P)H:quinone acceptor oxidoreductase 1; Nrf2, nuclear factor-erythroid 2-related factor-2; PAH, polycyclic aromatic hydrocarbon; RES, resveratrol; ROS, reactive oxygen species; TBF, terbinafine hydrochloride; TNF-α, tumor necrosis factor-α

Received 10 November 2010; revised 29 April 2011; accepted 13 May 2011; published online 14 July 2011

nuclear factor-erythroid 2-related factor-2 (Nrf2), which is a key molecule responsible for turning on the protective systems for cell damage. Nrf2 is anchored to Kelch-like ECH-associated protein 1 in the cytoplasm. When the Nrf2–Kelch-like ECH-associated protein 1 complex is disrupted by an inducer, Nrf2 translocates from the cytoplasm into the nucleus to bind antioxidant response elements (AREs). ARE-mediated induction of antioxidant enzymes, including NAD(P)H:quinone oxidoreductase 1 (Nqo1), is critical for protection from cell damage caused by reactive oxygen species (ROS; Jaiswal, 2004).

Therefore, we hypothesized that KCZ may exert its anti-inflammatory effects on inflammatory skin diseases by activating Nrf2 via AhR signaling. To prove this, cultured NHEKs were treated with KCZ. We demonstrated that KCZ (1) activates AhR signaling in NHEKs, (2) activates Nrf2 via AhR signaling, and (3) inhibits tumor necrosis factor-α (TNF-α)- or BaP-induced ROS and IL-8 production via AhR-Nrf2.

RESULTS

KCZ, terbinafine hydrochloride, BaP, and resveratrol do not affect NHEK viability

Cell viability was determined by Trypan blue dye exclusion. Incubation with KCZ (10 nM–1 μM), terbinafine hydrochloride (TBF; 1 μM), BaP (1 μM), and resveratrol (RES; 1 μM) for 48 hours showed no effect on the viability or morphological features of NHEKs (data not shown), as described previously (Kanda and Watanabe, 2006).

KCZ activates AhR signaling in NHEKs

To determine whether KCZ activates AhR signaling, we examined AhR nuclear translocation. NHEKs were treated with DMSO (control), KCZ (1 μM), or TBF (1 μM), a non-azole antifungal agent, for 6 hours. Confocal laser scanning micro scopy revealed that AhR was mainly localized in the cytoplasm under unstimulated condition (DMSO treatment; Figure 1a). Following KCZ treatment, AhR staining was observed mainly in the nuclei (Figure 1b), indicating that KCZ induces AhR nuclear translocation in NHEKs. In contrast, TBF treatment did not affect AhR distribution (Figure 1c) even after 24 hours (data not shown).

Next, we examined whether KCZ induced CYP1A1 expression by quantitative real-time PCR (qRT-PCR) and western blotting analysis. NHEKs were treated with KCZ (1 μM) for 3, 6, 24, and 48 hours for qRT-PCR analysis and for 24 and 48 hours for western blotting analysis. KCZ induced CYP1A1 mRNA and protein upregulation (Figure 1e and f). Furthermore, NHEKs were treated with different doses of KCZ (10 nM, 100 nM, and 1 μM) for 3 hours, because AhR began to translocate into the nuclei at this point (data not shown). KCZ induced the upregulation of CYP1A1 mRNA in a dose-

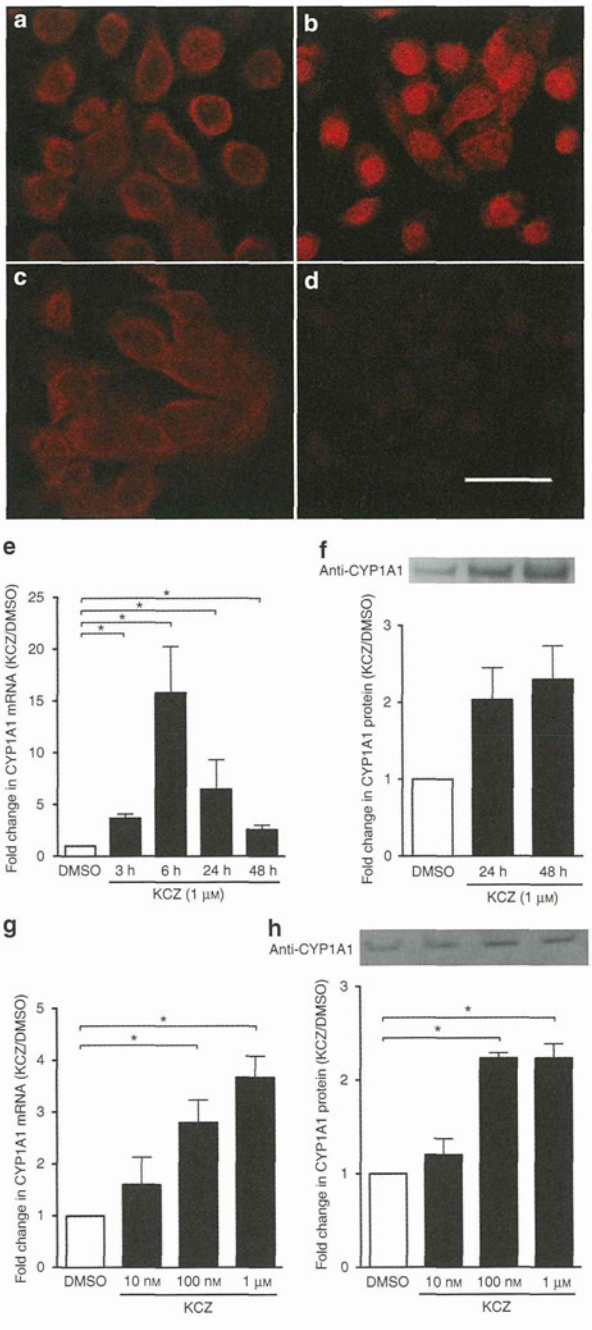

Figure 1. Ketoconazole (KCZ) activated aryl hydrocarbon receptor signaling in normal human epidermal keratinocytess. Confocal laser scanning microscopic analysis. (**a**) DMSO treatment (control), (**b**) KCZ (1 μM), (**c**) terbinafine hydrochloride (1 μM) treatment for 6 hours, and (**d**) isotype negative control. Bar = 50 μm. Representative data, $n = 3$ (**a**–**d**). (**e**, **g**) Quantitative real-time PCR analysis. Treatment with 1 μM KCZ for 3, 6, 24, and 48 hours or with 10 nM, 100 nM, and 1 μM KCZ for 3 hours. CYP1A1 mRNA levels normalized for glyceraldehyde-3-phosphate dehydrogenase (GAPDH) mRNA levels were expressed as fold induction compared with DMSO group. (**f**, **h**) Western blotting analysis. Treatment with 1 μM KCZ for 24 and 48 hours or with 10 nM, 100 nM, and 1 μM KCZ for 24 hours. CYP1A1 protein levels were normalized for GAPDH protein levels using ImageJ. Means ± SD, ($n = 3$) (**e**–**h**). *$P < 0.05$ (**e**–**h**).

dependent manner (Figure 1g). Western blotting analysis confirmed that KCZ induced the upregulation of CYP1A1 protein in NHEKs treated with KCZ (100 nM and 1 μM) for 24 or 48 hours (Figure 1h).

KCZ activates Nrf2 signaling in NHEKs

To elucidate whether KCZ activates Nrf2 in NHEKs, we examined Nrf2 distribution. NHEKs were treated with DMSO (control) or KCZ (1 μM) for 12 hours. Under unstimulated condition (DMSO treatment), Nrf2 was mainly localized in the cytoplasm (Figure 2a). Following KCZ treatment, Nrf2 staining was observed mainly in the nuclei (Figure 2b), indicating that KCZ induces Nrf2 nuclear translocation.

Next, we examined whether KCZ induced Nrf2 and Nqo1 upregulation. NHEKs were treated with KCZ for 12 hours for qRT-PCR analysis and for 24 hours for western blotting analysis. KCZ induced Nrf2 and Nqo1 mRNA and protein upregulation in a dose-dependent manner (Figure 2d and e).

Furthermore, ELISA-based Nrf2 transcriptional assay, which detects whether Nrf2 protein interacted with an oligonucleotide in ARE, confirmed that KCZ-induced nuclear Nrf2 bound to ARE (Figure 2f).

Nrf2 activation by KCZ requires AhR signaling in NHEKs

To examine whether KCZ activates Nrf2 via AhR signaling, AhR was knocked down by small interference (si)RNA transfection. After transfection with siRNA control (si-control) or siRNA against AhR (si-AhR) for 48 hours, NHEKs were treated with KCZ (1 μM) or BaP (1 μM) for 12 hours. KCZ induced Nrf2 nuclear translocation in si-control-transfected NHEKs (Figure 3a); however, in si-AhR-transfected NHEKs, the KCZ-induced Nrf2 nuclear translocation was completely abolished (Figure 3b). In addition, BaP induced Nrf2 upregulation in si-control-transfected NHEKs, which was inhibited in si-AhR-transfected NHEKs. However, BaP did not induce Nrf2 nuclear translocation (Supplementary Figure S1 online). Si-AhR transfection successfully knocked down AhR expression at the protein level (Figure 3d).

AhR and Nrf2 are responsible for the inhibitory effect of KCZ on TNF-α-induced ROS–IL-8 production

To evaluate the inhibitory effect of KCZ on inflammation, we used TNF-α to induce ROS-mediated IL-8 production in NHEKs (Young *et al.*, 2008). After treatment with DMSO (control) or KCZ (1 μM) for 48 hours, NHEKs were exposed to TNF-α (10 ng ml^{-1}) for 30 minutes. ROS production was evaluated using 2′,7′-dichlorofluorescein diacetate (DCFH-DA). DMSO (control; Figure 4a) and KCZ (1 μM) treatment for 6, 24, and 48 hours (Figure 4b) did not induce visible ROS production (Supplementary Figure S2 online). In contrast, TNF-α markedly induced ROS production in DMSO-treated NHEKs (control; Figure 4c), but not when NHEKs were treated with KCZ (Figure 4d).

Next, we examined whether KCZ exerted this anti-inflammatory effect by AhR-mediated gene expression, including AhR, Nrf2, and aryl hydrocarbon receptor repressor (AhRR) genes. AhRR functions as a negative feedback to AhR signaling, which inhibits CYP1A1 upregulation (Mimura *et al.*, 1999). TNF-α did not affect AhRR mRNA expression and KCZ-induced CYP1A1 upregulation (Supplementary Figure S3 online). siRNA transfection successfully knocked down Nrf2 expression at the protein level (Figure 3d) and AhRR expression at the mRNA level (Figure 4i). KCZ (1 μM) inhibited TNF-α-induced ROS in si-control (Figure 4e) or si-AhRR (Figure 4h)-transfected NHEKs, which was canceled in si-AhR (Figure 4f) or si-Nrf2 (Figure 4g)-transfected NHEKs.

Furthermore, we examined the effect of KCZ on IL-8 production (Figure 4, Supplementary Figure S4 online). After KCZ (100 nM, 1 μM) treatment for 48 hours, NHEKs were exposed to TNF-α (50 ng ml^{-1}) for 3 hours. KCZ inhibited TNF-α-induced IL-8 production in the culture supernatant in a dose-dependent manner (Figure 4j). More importantly, AhR or Nrf2 knockdown, but not AhRR knockdown, canceled this inhibitory effect on TNF-α-induced IL-8 production (Figure 4k).

KCZ inhibits BaP-induced oxidative stress in NHEKs

We hypothesized that KCZ might inhibit oxidative stress induced by AhR agonists, including PAHs and dioxins antagonistically, because KCZ also activates AhR signaling. After KCZ (100 nM, 1 μM) or DMSO (control) treatment for 48 hours, NHEKs were exposed to BaP (1 μM) for 24 hours. KCZ and BaP did not affect AhRR mRNA expression (Supplementary Figure S3 online). BaP induced ROS production in NHEKs (Figure 5b), which was inhibited by KCZ treatment (Figure 5c). Furthermore, Nrf2 (Figure 5e), but not AhRR (Figure 5f), knockdown canceled the inhibitory effect of KCZ on BaP-induced ROS production. Next, we examined whether KCZ inhibited BaP-induced IL-8 upregulation (Figure 5g, Supplementary Figure S4 online). KCZ (100 nM and 1 μM) inhibited BaP-induced IL-8 production in a dose-dependent manner (Figure 5g). Furthermore, we examined nuclear 8-hydroxydeoxyguanosine (8-OHdG) production resulting from DNA damage induced by ROS (Saladi *et al.*, 2003). KCZ (1 μM) treatment for 48 hours did not induce 8-OHdG production (data not shown). BaP (1 μM) exposure for 24 hours induced 8-OHdG production in DMSO-treated NHEKs (control), which was significantly inhibited by KCZ (100 nM, 1 μM) in a dose-dependent manner (Figure 5h).

DISCUSSION

The present study has provided the first evidence that KCZ induces Nrf2 activation in cultured human keratinocytes through AhR-dependent mechanisms. Specifically, we have demonstrated that KCZ induces Nrf2 nuclear translocation and promotes Nrf2 binding to ARE, leading to Nqo1 upregulation. Nqo1 is a relevant marker for Nrf2 activation (Marrot *et al.*, 2008), implying KCZ as an Nrf2 inducer and activator.

Our studies using siRNA targeted against AhR revealed that AhR is required to initiate Nrf2 translocation after KCZ treatment (Figure 3a and b). Recent data have provided lines of evidence regarding the cross-talk between AhR signaling and Nrf2, leading to the induction of antioxidant enzymes in human hepatocytes (Yeager *et al.*, 2009). They have suggested two possible mechanisms by which AhR signaling

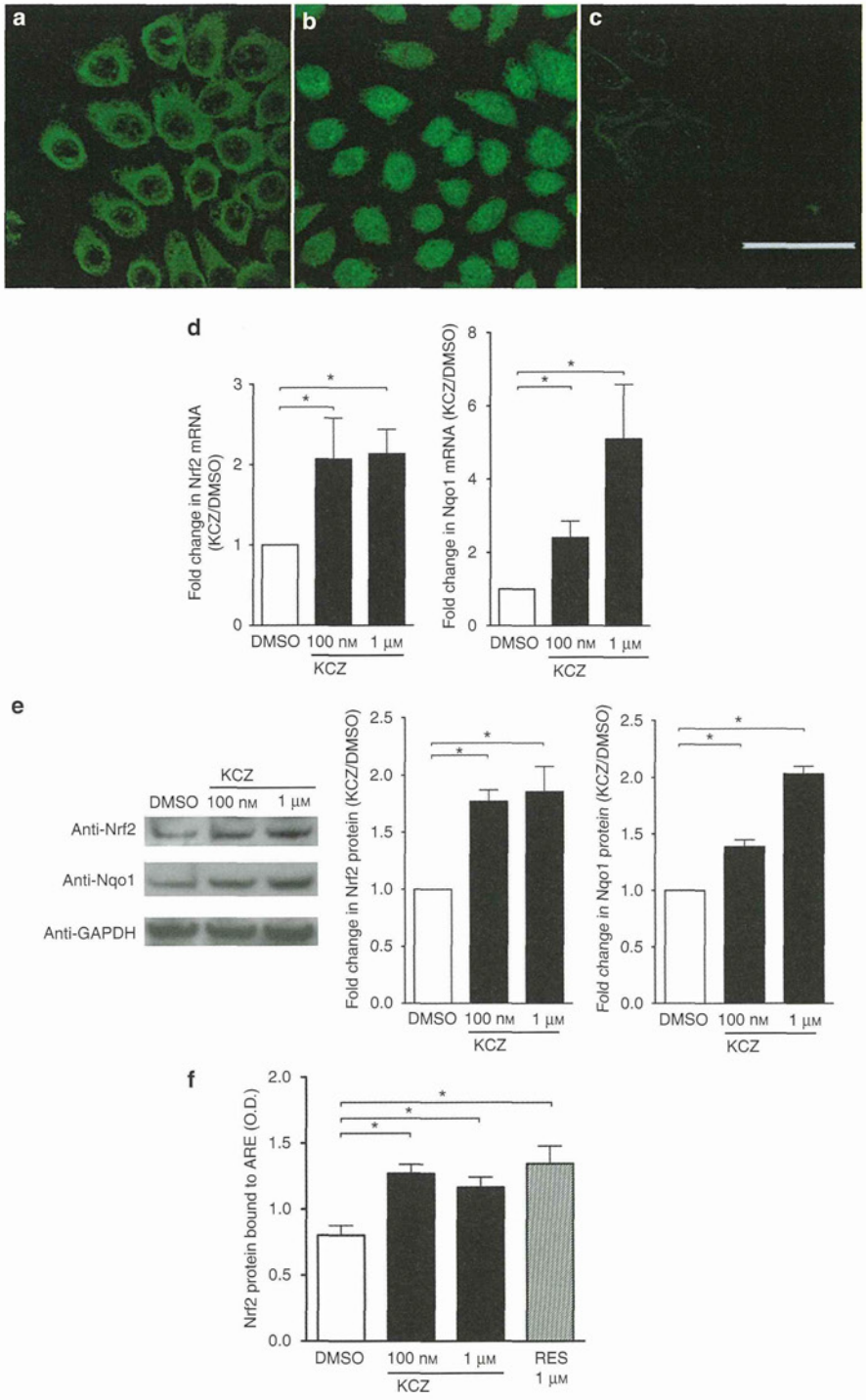

Figure 2. Ketoconazole (KCZ) activated nuclear factor-erythroid-2-related factor-2 (Nrf2) in normal human epidermal keratinocytes. Confocal laser scanning microscopic analysis. (**a**) DMSO treatment (control). (**b**) Treatment with 1 μM KCZ for 12 hours. (**c**) Isotype negative control. Bar = 50 μm. Representative data, $n = 3$ (**a**–**c**). (**d**) Quantitative real-time PCR analysis. Treatment with 100 nM and 1 μM KCZ for 12 hours. Nrf2 or Nqo1 mRNA levels normalized for glyceraldehyde-3-phosphate dehydrogenase (GAPDH) mRNA levels were expressed as fold induction compared with the DMSO group. (**e**) Western blotting analysis. Treatment with 100 nM and 1 μM KCZ for 24 hours. Protein levels were normalized for GAPDH protein levels using ImageJ. (**f**) ELISA-based Nrf2 transcriptional analysis. Protein levels of nuclear Nrf2, which interacted with an oligonucleotide in antioxidant response elements were measured. Data are presented as means ± SD, $n = 3$ (**d**–**f**). *$P < 0.05$ (**d**–**f**).

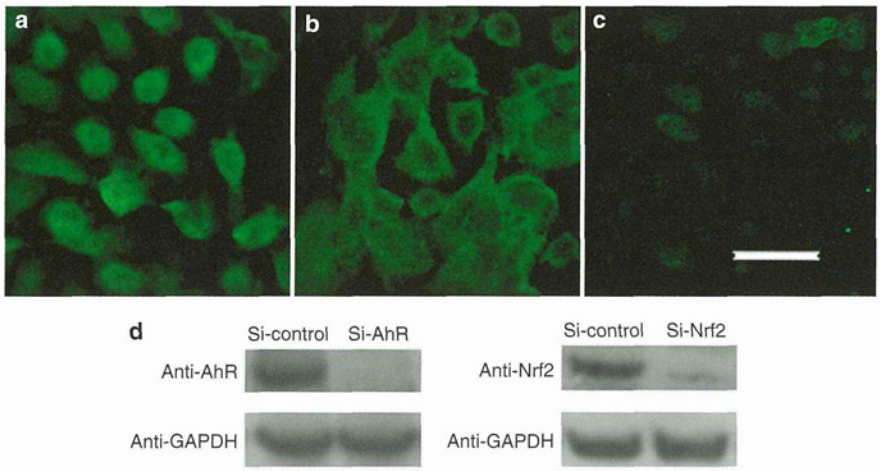

Figure 3. Ketoconazole (KCZ) activated nuclear factor-erythroid-2-related factor-2 (Nrf2) via aryl hydrocarbon receptor (AhR) signaling in normal human epidermal keratinocytes (NHEKs). After transfection with small interference (si) RNA control (si-control) or siRNA against AhR (si-AhR) for 48 hours, NHEKs were treated with 1 μM KCZ for 12 hours. Nrf2 distribution was observed by confocal laser scanning microscopy. (**a**) Si-control-transfected NHEKs. KCZ induced Nrf2 nuclear translocation as described in Figure 2b. (**b**) Si-AhR-transfected NHEKs. KCZ-induced Nrf2 nuclear translocation was completely abolished. (**c**) Isotype negative control. Bar = 50 μm. (**d**) Western blotting analysis. Si-AhR or si-Nrf2 transfection successfully knocked down AhR or Nrf2 expression at the protein level, respectively. Representative data, $n = 3$ (**a**–**d**). GAPDH, glyceraldehyde-3-phosphate dehydrogenase; RES, resveratrol.

activates Nrf2: (1) ROS production caused by CYP1A1 metabolism of a ligand would facilitate Nrf2 nuclear translocation and (2) AhR might bind to the Nrf2 gene locus and increase Nrf2 transcription as suggested by Miao *et al.* (2005). Our results possibly support the latter mechanism, because KCZ treatment did not induce ROS production (Figure 4b, Supplementary Figure S2 online). Although we showed that KCZ induced AhR nuclear translocation and CYP1A1 expression, we did not confirm the binding between KCZ and AhR in NHEKs. KCZ has been shown to directly bind to AhR and induce AhR nuclear translocation in human hepatocytes (Korashy *et al.*, 2007), indicating that KCZ may be a, to our knowledge, previously unreported AhR ligand. In addition, Henry and Gasiewicz (2008) have determined specific amino acids within AhR ligand-binding domains, showing that non-dioxin chemicals bind to AhR. These previous reports strongly suggest that KCZ activates AhR signaling in NHEKs through the direct engagement of KCZ to AhR.

Next, we have demonstrated that KCZ exerts an anti-inflammatory effect against TNF-α- or BaP-induced oxidative stress. Similar results that KCZ inhibits ROS released by primed inflammatory cells (Nakashima *et al.*, 2007) and TNF-α-induced CCL27, CCL12, and CCL5 production in NHEKs (Kanda and Watanabe, 2006) have been reported; however, the underlying molecular mechanism remains unknown. The present study has identified that AhR and Nrf2, but not AhRR, are critical in the anti-inflammatory effect of KCZ in NHEKs. The mRNA expression of AhRR, a negative feedback to AhR activation (Mimura *et al.*, 1999), was not affected by KCZ, TNF-α, and BaP (Supplementary Figure S3 online). Indeed, AhRR mRNA expression in NHEKs was much lower than that in HeLa cells and normal human dermal fibroblasts (NHDFs; Supplementary Figure S3 online; Tsuchiya *et al.*, 2003; Akintobi *et al.*, 2007), suggesting that AhRR does not modulate AhR activation sufficiently in NHEKs.

Results from AhR activation differ with cell types and AhR ligands. Whether AhR activation inhibits inflammation, including IL-8 expression, has remained controversial. In keratinocytes, AhR ligands affect responses of AhR activation strongly. 6-Formylindolo[3,2-b]carbazole, a tryptophan derivate, and 2,3,7,8-tetrachlorodibenzodioxin induce inflammation by AhR-mediated cyclooxygenase-2 induction (Fritsche *et al.*, 2007), whereas curcumin, a potent AhR activator (Rinaldi *et al.*, 2002), induces cyclooxygenase-2 inhibition (Nandal *et al.*, 2009). Furthermore, AhR translocated into nuclei by 2,3,7,8-tetrachlorodibenzodioxin exposure interacts with the NF-κ light-chain enhancer of the activated B-cell (NF-κB) subunit RelB and binds to a RelB/AhR-responsive element of IL-8 promoter (Vogel *et al.*, 2007). On the other hand, RES, which is another AhR ligand, inhibits NF-kB activation (Adhami *et al.*, 2003), although it induces AhR nuclear translocation (Casper *et al.*, 1999). Thus, the type of AhR ligand is an important factor in determining the response of AhR signaling. Some AhR ligands including RES (Liu *et al.*, 2011) and curcumin (Natarajan *et al.*, 2010) induce Nrf2 upregulation in human keratinocytes. Activation of Nrf2-antioxidant signaling attenuates NF-kB- or cyclooxygenase-2-induced inflammatory response (Li *et al.*, 2008; Hwang *et al.*, 2011). Therefore, we believe that the Nrf2 activation by AhR ligands contributes to the subsequent response of AhR signaling.

The property of KCZ to inhibit TNF-α-induced ROS and IL-8 production suggests that KCZ can be a therapeutic agent for various inflammatory skin diseases because ROS trigger the induction and maintenance of skin inflammation (Bickers and Athar, 2006) and IL-8 is a major proinflammatory

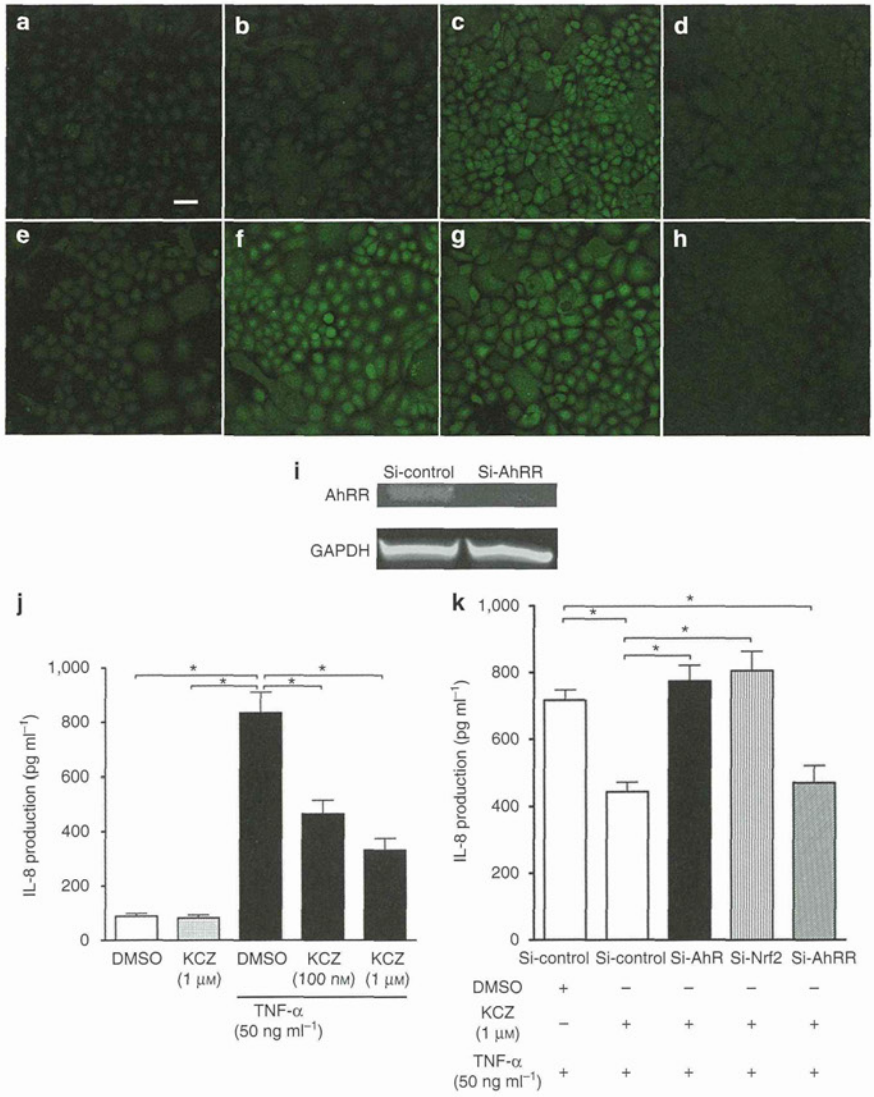

Figure 4. The inhibitory effect of ketoconazole (KCZ) on tumor necrosis factor-α (TNF-α)-induced reactive oxidative species (ROS)-IL-8 production required aryl hydrocarbon receptor (AhR) and nuclear factor-erythroid 2-related factor-2 (Nrf2). ROS production evaluation using 2′,7′-dichlorofluorescein diacetate. (**a**) DMSO (control), bar = 50 μm. (**b**) KCZ (1 μM, 48 hours). (**c**) TNF-α (10 ng ml^{-1}, 30 minutes) induced ROS production (**d**), but not in KCZ (100 nM, 48 hours)-pretreated normal human epidermal keratinocytes (NHEKs) (**e**). KCZ inhibited TNF-α-induced ROS production in si-control- (**e**) or si-aryl hydrocarbon receptor repressor (AhRR)- (**h**) transfected NHEKs, which was canceled in si-AhR- (**f**) or si-Nrf2- (**g**) transfected NHEKs. (**i**) Reverse transcription-PCR analysis. Small interference (si)-aryl hydrocarbon receptor repressor (AhRR) transfection successfully knocked down AhRR mRNA expression. Representative data, $n = 3$ (**a-i**). (**j**) KCZ pretreatment (48 h) inhibited tumor necrosis factor-α (TNF-α; 50 ng ml^{-1}, 3 hours)-induced IL-8 production in a dose-dependent manner. (**k**) KCZ inhibited TNF-α-induced IL-8 production in si-control- or si-AhRR-transfected NHEKs, but not in si-AhR- or si-Nrf2-transfected NHEKs. Data are presented as means ± SD, $n = 3$ (**j**, **k**). *$P < 0.05$ (**j**, **k**).GAPDH, glyceraldehyde-3-phosphate dehydrogenase.

cytokine/chemokine activating the recruitment and function of neutrophils (Baggiolini and Clark-Lewis, 1992). Furthermore, considering that AhR signaling is originally a metabolizing system for PAHs, we evaluated the property of KCZ to inhibit oxidative stress caused by an AhR agonist, including PAHs. KCZ inhibited BaP-induced ROS, IL-8, and 8-OHdG production (Figure 5c, d, g and h). 8-OHdG is a marker of DNA damage caused by ROS contributing to carcinogenesis (Saladi *et al.*, 2003). Elucidation of the precise molecular mechanism by which KCZ inhibits BaP-induced oxidative stress appears quite difficult in this system, because BaP also activates AhR signaling in NHEKs. However, Nrf2 knockdown restored the inhibitory effect of KCZ on BaP-induced ROS production, suggesting that Nrf2 possibly has an important role. These data suggest that KCZ may protect cells from AhR-mediated oxidative stress, including PAHs

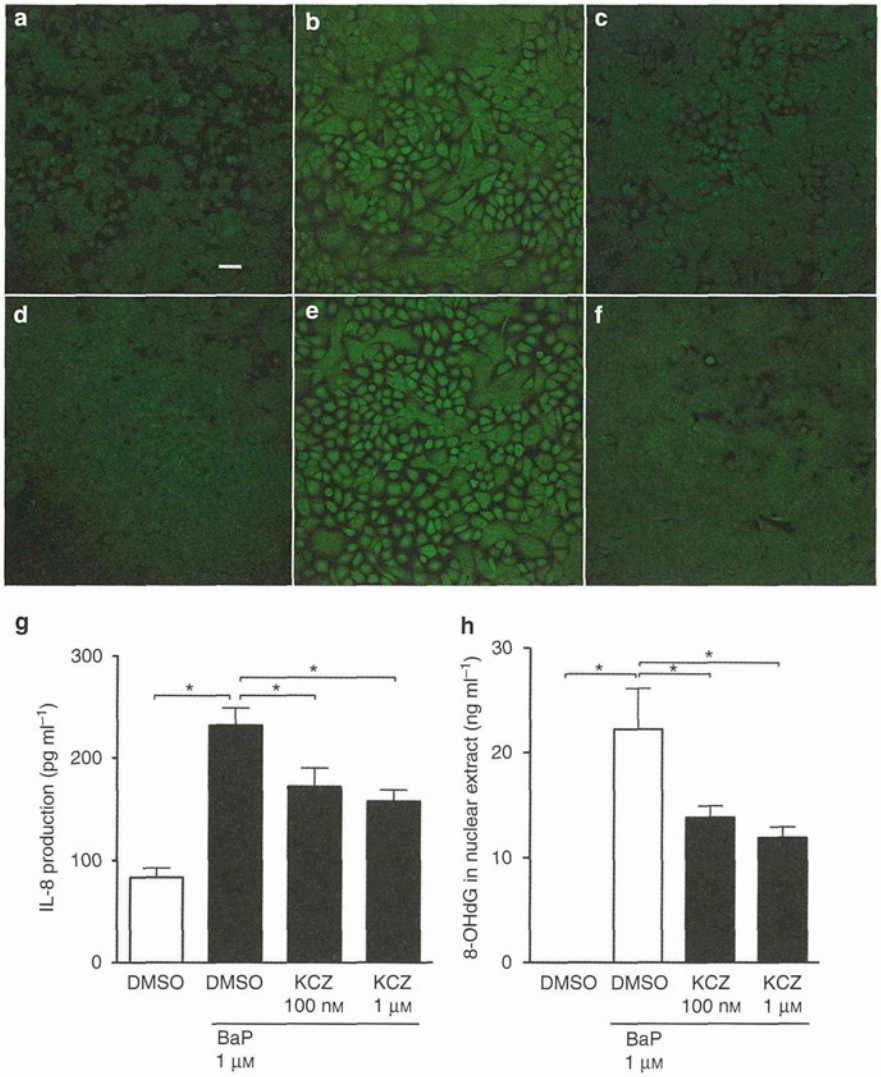

Figure 5. Ketoconazole (KCZ) inhibited benzo(a)pyrene (BaP)-induced reactive oxidative species (ROS)-IL-8 production in normal human epidermal keratinocytes (NHEKs). ROS production evaluation using 2′,7′-dichlorofluorescein diacetate. (**a**) DMSO (control), bar = 50 μm. BaP (1 μM) treatment for 24 hours induced ROS production (**b**), which was inhibited by KCZ (100 nM) pretreatment for 48 hour-treated NHEKs (**c**). Si-Nrf2 transfection (**e**) canceled this KCZ inhibition, but si-control (**d**) and small interference (si)-aryl hydrocarbon receptor repressor (**f**) transfection did not. Representative data, $n = 3$ (**a–f**). (**g**) ELISA: IL-8 production in culture supernatant. BaP induced IL-8 production in DMSO-treated NHEKs (control), which was inhibited by KCZ treatment in a dose-dependent manner. (**h**) ELISA: 8-hydroxydeoxyguanosine (8-OHdG) production in nuclear extract. BaP induced 8-OHdG production in DMSO (control)-treated NHEKs, which was inhibited by KCZ treatment in a dose-dependent manner. Data are presented as means ± SD, $n = 3$ (**g**, **h**). *$P < 0.05$ (**g**, **h**).
Nrf2, nuclear factor-erythroid 2-related factor-2.

and dioxin toxicity. As AhR-mediated oxidative stress is partly involved in clinical symptoms of dioxin-overexposed patients, including Yucheng (Wang *et al.*, 2008) and Yusho patients (Imamura *et al.*, 2007), KCZ treatment may have a possibility to improve these symptoms.

We found that 100 nM KCZ was sufficient to inhibit ROS and IL-8 production. The concentration of 100 nM is much lower than the peak serum concentration (7.2 μM) obtained from oral KCZ (200 mg) treatment (Chin *et al.*, 1995). As oral KCZ occasionally causes hepatic dysfunction, topical skin application is used more frequently, suggesting that the KCZ dose obtained from topical treatment is desirable for *in vitro* assay. However, to the best of our knowledge, there are still no studies that indicate the optimal KCZ dose based on topical treatment. Molecules with a molecular weight under 500 Da can penetrate normal skin (Bos and Meinardi, 2000). KCZ, having a molecular weight of 531 Da, may thus partially penetrate normal skin. However, KCZ absorption may be increased in an inflamed skin because the inflammation impairs the skin barrier function.

In conclusion, our findings suggest that engagement of AhR by KCZ induces the cytoprotective effect mediated by Nrf2 activation, which potently downregulates either cytokine-induced (AhR-independent) or PAH-induced (AhR-dependent) oxidative stress in cultured human keratinocytes.

MATERIALS AND METHODS

Regents and antibodies

KCZ, RES, TBF, BaP, and DMSO were purchased from Sigma Chemical (St Louis, MO). TNF-α was obtained from Peprotech (Rocky Hill, NJ). Anti-AhR rabbit polyclonal IgG antibody (H-211), anti-CYP1A1 mouse monoclonal IgG antibody (B-4), anti-Nrf2 polyclonal rabbit IgG antibody (H-300), anti-AhRR rabbit IgG antibody (D-14), anti-glyceraldehyde-3-phosphate dehydrogenase (GAPDH) rabbit IgG antibody (FL-335), normal rabbit IgG, and normal mouse IgG were obtained from Santa Cruz Biotechnology (Santa Cruz, CA). Anti-Nqo1 mouse monoclonal IgG (A180) was procured from Abcam (Cambridge, UK).

Cell culture

NHEKs, NHDFs, obtained from Clonetics-BioWhittaker (San Diego, CA), and HeLa cells (CCL-2, ATCC) were grown in culture dishes at 37 °C, 5% CO_2. NHEKs were cultured in serum-free keratinocyte growth medium (Lonza, Walkersville, MD) supplemented with bovine pituitary extract, recombinant epidermal growth factor, insulin, hydrocortisone, transferrin, and epinephrine. NHDFs and HeLa cells were cultured in DMEM supplemented with 10% fetal calf serum, 2 mM non-essential amino-acid solution, 2 mM pyruvate, and 2 mM HEPES buffer. Culture medium was replaced every 2 days. At near confluence (70–90%), cells were disaggregated with 0.25% trypsin/0.01% ethylenediamine tetraacetic acid and subcultured. Second-to-fourth-passage NHEKs or NHDFs were uszed in all experiments.

Treatment of cultured NHEKs

NHEKs (1×10^5) were seeded in 24-well culture plates, allowed to attach for 24 hours, and subsequently treated with KCZ, TBF, RES, BaP, TNF-α, or DMSO. Various concentrations of KCZ (10 nM, 100 nM and 1 μM), TBF (1 μM), RES (1 μM), BaP (1 μM), and TNF-α (10 or 50 ng ml^{-1}) were prepared in cell culture medium. Control cultures received medium containing a comparable DMSO concentration (up to 0.05%). Fresh medium containing KCZ, TBF, RES, BaP, TNF-α, or DMSO was added as indicated in the figure legend.

Immunofluorescence and confocal laser scanning microscopic analysis

NHEKs cultured on slides were washed in phosphate-buffered saline (PBS), fixed with acetone for 10 minutes, and blocked using 10% BSA in PBS for 30 minutes. Samples were incubated with primary rabbit anti-AhR (1:50) or rabbit anti-Nrf2 (1:50) in PBS overnight at 4 °C. Slides were washed in PBS before incubation with anti-rabbit (Alexa Fluor 488 or 546, Molecular Probes, Eugene, OR) secondary antibody for 1.5 hours at room temperature. Slides were mounted with ProLong Gold antifade reagent (Invitrogen, Carlsbad, CA). All samples were analyzed using D-Eclipse confocal laser scanning microscope (Nikon, Tokyo, Japan).

Reverse transcription-PCR and qRT-PCR analyses

Total RNA was extracted using RNeasy Mini kit (Qiagen, Valencia, CA). Reverse transcription was performed using PrimeScript RT-PCR kit (Takara Bio, Shiga, Japan). Amplification was started at 95 °C for 10 seconds as the first step, followed by 35 cycles of PCR at 95 °C for 5 seconds, and at 60 °C for 20 seconds. PCR products were analyzed using electrophoresis, and densitometric analysis was performed using ImageJ software (NIH). ImageJ is a public domain, Java-based image processing program developed at the National Institutes of Health (NIH; Bethesda, MD). qRT-PCR was performed on the Mx3000p real-time system (Stratagene, La Jolla, CA) using SYBR Premix Ex Taq (Takara Bio). The amplification protocol was the same as that with reverse transcription-PCR. mRNA expressions were measured in triplicate and were normalized for GAPDH expression levels. The primers from Takara Bio and SABiosciences (Frederick, MD) were as follows: AhR: forward 5′-ATCACCTACGCCAGTCGCA AG-3′ and reverse: 5′-AGGCTAGCCAAACGGTCCAAC-3′; Nrf2: forward 5′-CTTGGCCTCAGTGATTCTGAAGTG-3′ and reverse: 5′-C CTGAGATGGTGACAAGGGTTGTA-3′; Nqo1: forward 5′-GGATTG GACCGAGCTGGAA-3′ and reverse: 5′-AATTGCAGTGAAGATGAA GGCAAC-3′; AhRR: forward 5′-GCCTCTGGGCATTTATGGATTTA AG-3′ and reverse: 5′-CTGGGCACTCGGTTAGAATAGGAA-3′; IL-8: forward 5′-ACTTTCAGAGACAGCAGAGCACACA-3′ and reverse: 5′-CCTTCACACAGAGCTGCAGAAATC-3′; and GAPDH: forward 5′-GCACCGTCAAGGCTGAGAAC-3′ and reverse: 5′-TGGTGAAGA CGCCAGTGGA-3′.

The CYP1A1 primers were PPH01271E (SABiosciences).

Western blotting analysis

NHEKs were incubated with lysis buffer (Complete Lysis-M, Roche Applied Science, Indianapolis, IN). Lysate protein concentration was measured using BCA Protein Assay kit (Pierce, Rockford, IL). Equal amounts of protein (40 μg) were dissolved in NuPage LDS Sample Buffer (Invitrogen) and 10% NuPage Sample Reducing Agent (Invitrogen). Lysates were boiled at 70 °C for 10 minutes and loaded and run on 4–12% NuPage Bis-Tris Gels (Invitrogen) at 200 V for 40 minutes. The proteins were transferred onto polyvinylidene fluoride membranes (Invitrogen) and blocked in 2% BSA in 0.1% Tween-20 (Sigma-Aldrich) and Tris-buffered saline. Membranes were probed with anti-AhR, anti-CYP1A1, anti-Nrf2, anti-AhRR, or anti-Nqo1 antibodies overnight at 4 °C. The secondary antibody used was anti-rabbit or anti-mouse horseradish peroxidase-conjugated IgG antibody. Protein bands were detected using the Western Breeze kit (Invitrogen). Densitometric analysis of protein band was performed using ImageJ software (NIH).

Detection of ROS production

DCFH-DA (Molecular Probes) is a cell-permeable non-fluorescent probe that is de-esterified intracellularly and oxidized to highly fluorescent 2′,7′-dichlorofluorescein in the presence of ROS. NHEKs were incubated with DCFH-DA (5 μM) for 30 minutes at 37 °C, and the fluorescence signal of 2′,7′-dichlorofluorescein (Ex = 490 nm), the oxidation product of DCFH-DA, was analyzed using a D-Eclipse confocal laser scanning microscope (Nikon).

ELISA

An IL-8 ELISA kit (Invitrogen) and a highly sensitive 8-OHdG ELISA kit (Japan Institute for the Control of Aging, Shizuoka, Japan)

were used according to the manufacturer's protocol. Nuclear proteins from NHEKs were extracted using NE-PER Nuclear and Cytoplasmic Extraction Reagents (Thermo Scientific, Rockford, IL). Optical density was measured using Labsystems Multiskan MS Analyzer (Thermo Bionalysis Japan, Tokyo, Japan).

ELISA-based Nrf2 transcriptional assay

Protein levels of Nrf2 interacted with an oligonucleotide contained in ARE were measured by TransAM Nrf2 (Active Motif, Carlsbad, CA). After KCZ treatment for 12 hours, nuclear extracts (10 μg) from NHEKs were used as samples. Optical density was measured using Labsystems Multiskan MS Analyzer (Thermo Bionalysis Japan).

Transfection with AhR, Nrf2, or AhRR-targeted specific small interference RNA

SiRNA targeted against AhR (si-AhR, s1200), Nrf2 (si-Nrf2, s9492) and AhRR (si-AhRR, s22144) and siRNA consisting of a scrambled sequence that would not lead to specific degradation of any cellular message (si-control) were purchased from Ambion (Austin, TX). NHEKs cultured in 24-well plates were incubated with mix from HiPerFect Transfection kit (Qiagen, Courtaboeuf, France) containing 10 nM siRNA and 3.0 μl of HiPerFect reagent in 0.5 ml of culture medium. After a 48-hour incubation period, siRNA-transfected NHEKs were treated with KCZ for 48 hours. siRNA transfection showed no effect on cell viability, as demonstrated by microscopic examination (data not shown).

Statistical analysis

Unpaired Student's *t*-test was used to analyze results, and a *P*-value <0.05 was considered to indicate a statistically significant difference.

CONFLICT OF INTEREST

The authors state no conflict of interest.

ACKNOWLEDGMENTS

This study was supported by a grant from the Ministry of Health, Labour, and Welfare, Japan, and the Environmental Technology Development Fund of the Ministry of the Environment, Japan.

SUPPLEMENTARY MATERIAL

Supplementary material is linked to the online version of the paper at http://www.nature.com/jid

REFERENCES

Adhami VM, Afaq F, Ahmad N (2003) Suppression of ultraviolet B exposure-mediated activation of NF-kappaB in normal human keratinocytes by resveratrol. *Neoplasia* 5:74–82

Akintobi AM, Villano CM, White LA (2007) 2,3,7,8-Tetrachlorodibenzo-p-dioxin (TCDD) exposure of normal human dermal fibroblasts results in AhR-dependent and -independent changes in gene expression. *Toxicol Appl Pharmacol* 220:9–17

Bäck O, Scheynius A, Johansson SG (1995) Ketoconazole in atopic dermatitis: therapeutic response is correlated with decrease in serum IgE. *Arch Dermatol Res* 287:448–51

Baggiolini M, Clark-Lewis I (1992) Interleukin-8, a chemotactic and inflammatory cytokine. *FEBS Lett* 307:97–101

Bickers DR, Athar M (2006) Oxidative stress in the pathogenesis of skin disease. *J Invest Dermatol* 126:2565–75

Bos JD, Meinardi MM (2000) The 500 Dalton rule for the skin penetration of chemical compounds and drugs. *Exp Dermatol* 9:165–9

Casley WL, Ogrodowczyk C, Larocque L *et al.* (2007) Cytotoxic doses of ketoconazole affect expression of a subset of hepatic genes. *J Toxicol Environ Health A* 70:1946–55

Casper RF, Quesne M, Rogers IM *et al.* (1999) Resveratrol has antagonist activity on the aryl hydrocarbon receptor: implications for prevention of dioxin toxicity. *Mol Pharmacol* 56:784–90

Chin TW, Loeb M, Fong IW (1995) Effects of an acidic beverage (Coca-Cola) on absorption of ketoconazole. *Antimicrob Agents Chemother* 39:1671–5

Darabi K, Hostetler SG, Bechtel MA *et al.* (2009) The role of Malassezia in atopic dermatitis affecting the head and neck of adults. *J Am Acad Dermatol* 60:125–36

De Pedrini P, Rapisarda R, Spanò G (1988) The effect of ketoconazole on sebum secretion in patients suffering from acne and seborrhea. *Int J Tissue React* 10:111–3

Farr PM, Krause LB, Marks JM *et al.* (1985) Response of scalp psoriasis to oral ketoconazole. *Lancet* 2:921–2

Fritsche E, Schäfer C, Calles C *et al.* (2007) Lightening up the UV response by identification of the aryl hydrocarbon receptor as a cytoplasmatic target for ultraviolet B radiation. *Proc Natl Acad Sci USA* 104:8851–6

Gupta AK, Nicol K, Batra R (2004) Role of antifungal agents in the treatment of seborrheic dermatitis. *Am J Clin Dermatol* 5:417–22

Haarmann-Stemmann T, Bothe H, Abel J (2009) Growth factors, cytokines and their receptors as downstream targets of aryl hydrocarbon receptor (AhR) signaling pathways. *Biochem Pharmacol* 77:508–20

Henry EC, Gasiewicz TA (2008) Molecular determinants of species-specific agonist and antagonist activity of a substituted flavone towards the aryl hydrocarbon receptor. *Arch Biochem Biophys* 472:77–88

Hwang YP, Choi JH, Yun HJ *et al.* (2011) Anthocyanins from purple sweet potato attenuate dimethylnitrosamine-induced liver injury in rats by inducing Nrf2-mediated antioxidant enzymes and reducing COX-2 and iNOS expression. *Food Chem Toxicol* 49:93–9

Imamura T, Kanagawa Y, Matsumoto S *et al.* (2007) Relationship between clinical features and blood levels of pentachlorodibenzofuran in patients with Yusho. *Environ Toxicol* 22:124–31

Jaiswal AK (2004) Nrf2 signaling in coordinated activation of antioxidant gene expression. *Free Radic Biol Med* 36:1199–207

Khan IU, Bickers DR, Haqqi TM *et al.* (1992) Induction of CYP1A1 mRNA in rat epidermis and cultured human epidermal keratinocytes by benz(a) anthracene and beta-naphthoflavone. *Drug Metab Dispos* 20:620–4

Kanda N, Watanabe S (2006) Suppressive effects of antimycotics on tumor necrosis factor-alpha-induced CCL27, CCL2, and CCL5 production in human keratinocytes. *Biochem Pharmacol* 72:463–73

Köhle C, Bock KW (2007) Coordinate regulation of phase I and II xenobiotic metabolisms by the Ah receptor and Nrf2. *Biochem Pharmacol* 73:1853–62

Korashy HM, Shayeganpour A, Brocks DR *et al.* (2007) Induction of cytochrome P450 1A1 by ketoconazole and itraconazole but not fluconazole in murine and human hepatoma cell lines. *Toxicol Sci* 97:32–43

Li W, Khor TO, Xu C *et al.* (2008) Activation of Nrf2-antioxidant signaling attenuates NFkappaB-inflammatory response and elicits apoptosis. *Biochem Pharmacol* 76:1485–9

Liu Y, Chan F, Sun H *et al.* (2011) Resveratrol protects human keratinocytes HaCaT cells from UVA-induced oxidative stress damage by down-regulating Keap1 expression. *Eur J Pharmacol* 10:130–7

Ma Q, Lu AY (2003) Origins of individual variability in P4501A induction. *Chem Res Toxicol* 16:249–60

Marrot L, Jones C, Perez P *et al.* (2008) The significance of Nrf2 pathway in (photo)-oxidative stress response in melanocytes and keratinocytes of the human epidermis. *Pigment Cell Melanoma Res* 21:79–88

Miao W, Hu L, Scrivens PJ *et al.* (2005) Transcriptional regulation of NF-E2 p45-related factor (NRF2) expression by the aryl hydrocarbon receptor-xenobiotic response element signaling pathway: direct cross-talk between phase I and II drug-metabolizing enzymes. *J Biol Chem* 280: 20340–8

Mimura J, Ema M, Sogawa K *et al.* (1999) Identification of a novel mechanism of regulation of Ah (dioxin) receptor function. *Genes Dev* 13:20–5

Nakashima T, Sato E, Niwano Y *et al.* (2007) Inhibitory or scavenging action of ketoconazole and ciclopiroxolamine against reactive oxygen species released by primed inflammatory cells. *Br J Dermatol* 156:720–7

Nandal S, Dhir A, Kuhad A *et al.* (2009) Curcumin potentiates the anti-inflammatory activity of cyclooxygenase inhibitors in the cotton pellet granuloma pouch model. *Methods Find Exp Clin Pharmacol* 31:89–93

Natarajan VT, Singh A, Kumar AA *et al.* (2010) Transcriptional upregulation of Nrf2-dependent phase II detoxification genes in the involved epidermis of vitiligo vulgaris. *J Invest Dermatol* 130:2781–9

Rinaldi AL, Morse MA, Fields HW *et al.* (2002) Curcumin activates the aryl hydrocarbon receptor yet significantly inhibits (−)-benzo(a)pyrene-7R-trans-7,8-dihydrodiol bioactivation in oral squamous cell carcinoma cells and oral mucosa. *Cancer Res* 62:5451–6

Saladi R, Austin L, Gao D *et al.* (2003) The combination of benzo[a]pyrene and ultraviolet A causes an *in vivo* time-related accumulation of DNA damage in mouse skin. *Photochem Photobiol* 77:413–9

Tsuchiya Y, Nakajima M, Itoh S *et al.* (2003) Expression of aryl hydrocarbon receptor repressor in normal human tissues and inducibility by polycyclic aromatic hydrocarbons in human tumor-derived cell lines. *Toxicol Sci* 72:253–9

Tsuji G, Takahara M, Uchi H *et al.* (2011) An environmental contaminant, benzo(a)pyrene, induces oxidative stress-mediated interleukin-8 production in human keratinocytes via the aryl hydrocarbon receptor signaling pathway. *J Dermatol Sci* 62:42–9

Vogel CF, Sciullo E, Li W *et al.* (2007) RelB, a new partner of aryl hydrocarbon receptor-mediated transcription. *Mol Endocrinol* 21:2941–55

Wang SL, Tsai PC, Yang CY *et al.* (2008) Increased risk of diabetes and polychlorinated biphenyls and dioxins: a 24-year follow-up study of the Yucheng cohort. *Diabetes Care* 31:1574–9

Yeager RL, Reisman SA, Aleksunes LM *et al.* (2009) Introducing the "TCDD-inducible AhR-Nrf2 gene battery". *Toxicol Sci* 111:238–46

Young CN, Koepke JI, Terlecky LJ *et al.* (2008) Reactive oxygen species in tumor necrosis factor-alpha-activated primary human keratinocytes: implications for psoriasis and inflammatory skin disease. *J Invest Dermatol* 128:2606–14

Journal of Dermatological Science 66 (2012) 37–43

Contents lists available at SciVerse ScienceDirect

Journal of Dermatological Science

journal homepage: www.elsevier.com/jds

Topically applied semaphorin 3A ointment inhibits scratching behavior and improves skin inflammation in NC/Nga mice with atopic dermatitis

Osamu Negi [a,1], Mitsutoshi Tominaga [a,c,1], Suhandy Tengara [a], Atsuko Kamo [a], Kenichi Taneda [b], Yasushi Suga [b], Hideoki Ogawa [a], Kenji Takamori [a,b,*]

[a] *Institute for Environmental and Gender Specific Medicine, Juntendo University Graduate School of Medicine, 2-1-1 Tomioka, Urayasu, Chiba 279-0021, Japan*
[b] *Department of Dermatology, Juntendo University Urayasu Hospital, 2-1-1 Tomioka, Urayasu, Chiba 279-0021, Japan*
[c] *Department of Neurobiology, Physiology and Behavior, University of California Davis, CA, United States*

ARTICLE INFO

Article history:
Received 19 December 2011
Accepted 13 January 2012

Keywords:
Atopic dermatitis
Epidermal keratinocytes
Nerve fibers
Pruritus
Sema3A

ABSTRACT

Background: Epidermal hyperinnervation in atopic dermatitis (AD) is activated directly by various external stimuli, causing enhanced itching. Nerve density is regulated by the nerve repulsion factor semaphorin 3A (Sema3A), along with nerve elongation factors.
Objective: To investigate the effects of Sema3A ointment in the NC/Nga mouse model of AD.
Methods: An AD-like phenotype was induced by repeated application of *Dermatophagoides farinae* body (Dfb) ointment to the dorsal skin of NC/Nga mice. Vaseline, heparinoid, betamethasone, tacrolimus and recombinant Sema3A ointments were applied to the lesional skin once a day for 4 days. Transepidermal water loss (TEWL) was measured before and after each treatment. We also scored the degree of dermatitis and recorded videos to observe scratching behavior. Subsequently, we collected skin samples from these mice for histological analyses.
Results: Topical application of Sema3A, betamethasone and tacrolimus ointments significantly inhibited scratching behavior and improved dermatitis scores in Dfb-treated mice compared with control mice, whereas vaseline and heparinoid had no effects. A significant improvement of TEWL was observed only in Sema3A ointment-treated mice. Moreover, Sema3A ointment reduced the densities of PGP9.5- and substance P-immunoreactive nerve fibers in the epidermis and the numbers of inflammatory cells, such as CD4 immunoreactive T cells and eosinophils, and improved acanthosis in the Dfb-treated mice compared with controls.
Conclusion: Sem3A ointment may have therapeutic efficacy in patients with pruritus and dermatitis of AD.

1. Introduction

Pruritus (or itching), an unpleasant sensation associated with the desire to scratch, frequently accompanies a variety of inflammatory skin conditions and systemic diseases. Histamine is the best-known pruritogen in humans and is also regarded as an experimental itch-causing substance. Clinically, antihistamines, *i.e.*, histamine H_1 antagonists, are commonly used to treat all types of itching resulting from renal and liver diseases, as well as from serious skin diseases, such as atopic dermatitis (AD). However, antihistamines often lack efficacy in patients with chronic itching [1–3].

Antihistamine-resistant itch may be caused by intraepidermal nerve fibers, suggesting that lesional skin is susceptible to stimulation and sensitive to itching [2,3]. The sprouting of epidermal nerve fibers associated with pruritus is found in human patients with AD [2,4], as well as in animal models of this condition [5,6]. Nerve growth factor (NGF) produced by keratinocytes is one of the major growth factors that determines skin innervations [2]. Increased plasma concentrations of NGF have been found to correlate with the severity of disease in patients with AD [2]. In addition, decreased concentrations of the nerve repulsion factor

Abbreviations: AD, atopic dermatitis; BSA, bovine serum albumin; Dfb, *Dermatophagoides farinae* body; DFS, direct fast scarlet 4BS; HE, hematoxylin–eosin; NDS, normal donkey serum; NGF, nerve growth factor; Nrp, neuropilin; OCT, optimal cutting temperature; PBS, phosphate-buffered saline; PBS-T, PBS containing Tween 20; PFA, paraformaldehyde; PGP9.5, protein gene product 9.5; Sema3A, semaphorin 3A; SDS, sodium dodecyl sulphate; SP, substance P; TB, toluidine blue; TEWL, transepidermal water loss; VEGF, vascular endothelial growth factor.

* Corresponding author. Tel.: +81 47 353 3171; fax: +81 47 353 3178.
E-mail address: ktakamor@juntendo.ac.jp (K. Takamori).

[1] These authors contributed equally to this work.

0923-1811/$36.00 © 2012 Japanese Society for Investigative Dermatology. Published by Elsevier Ireland Ltd. All rights reserved.
doi:10.1016/j.jdermsci.2012.01.007

epidermal semaphorin 3A (Sema3A) have been reported in AD patients [7]. Sema3A has been shown to inhibit NGF-induced sprouting of sensory afferents in the adult rat spinal cord [8], whereas elevated NGF concentrations have been found to reduce the Sema3A-induced collapse of sensory growth cones [9]. These findings have suggested that axonal guidance molecules, such as NGF and Sema3A, are pivotal in regulating epidermal hyperinnervation. Sema3A may therefore be a therapeutic target for ameliorating pruritus associated with epidermal nerve density, such as AD. We have therefore assessed whether ointment containing Sema3A is effective against pruritus and inflammation associated with the AD-like phenotype in NC/Nga mice.

2. Materials and methods

2.1. Animals

Specific pathogen-free male NC/Nga mice, aged 10–12 weeks, were purchased from Charles River Japan (Yokohama, Japan) and housed in an animal room under conditions of controlled temperature (22–24 °C), humidity (50 ± 5%) and light (lights on 08:00–20:00). Food and tap water were provided *ad libitum*. All animal procedures were approved by the institutional Animal Care and Use Committee at Juntendo University Graduate School of Medicine and conformed to the Guidelines for the Use of Laboratory Animals of the National Institutes of Health.

2.2. Reagents

Recombinant human Sema3A (rhSema3A) was purchased from R&D Systems (Minneapolis, MN, USA), hydrophilic petrolatum (vaseline, ointment base) from Maruishi (Osaka, Japan), *Dermatophagoides farinae* body (Dfb) ointment (Biostir-AD) from Biostir Inc. (Kobe, Japan), heparinoid cream (Hirudoid® Soft) from Maruho Inc. (Osaka, Japan), betamethasone dipropionate (Rinderon®DP) from Shionogi & Co., Ltd. (Osaka, Japan), and tacrolimus (Protopic®) from Astellas Pharma Inc. (Tokyo, Japan). Optimal cutting temperature (OCT) compound was obtained from Sakura Finetechnical Co., Ltd. (Tokyo, Japan), normal donkey serum (NDS) from Chemicon (Temecula, CA, USA), bovine serum albumin (BSA) from Sigma (St. Louis, MO, USA), Vectashield® mounting medium from Vector Laboratories Ltd. (Peterborough, UK) and sevoflurane from Abbott Japan (Osaka, Japan).

2.3. Antibodies

Rabbit anti-protein gene product 9.5 (PGP9.5, 1:4000 dilution) was from Biomol International Corp. (Plymouth Meeting, PA, USA), rat anti-substance P (SP, 1:100 dilution) was from (Chemicon), rabbit anti-NGF (1:500 dilution) was from Millipore Corp. (Billerica, MA, USA), rabbit anti-Sema3A (1:200 dilution) was from Abcam Inc. (Cambridge, MA, UK) and rat anti-CD4 (1:50 dilution) was from Santa Cruz Biotechnology (Santa Cruz, CA, USA). Secondary antibodies conjugated with Alexa Fluor dye (1:300 dilution) were purchased from Molecular Probes (Eugene, OR, USA).

2.4. Induction of dermatitis in NC/Nga mice

Dermatitis was induced in NC/Nga mice as described [10]. On day 0, the mice were anesthetized with sevoflurane, the rostral part of the back skin was clipped with an electric shaver, and residual hair was depilated using a hair removal cream. Ointment containing 100 mg Dfb or ointment base alone (Vaseline) was topically applied to the shaved dorsal skin. For the second induction, growing hair was removed with an electric shaver, followed by barrier disruption by treatment of the shaved dorsal skin with 150 μL of 4% sodium dodecyl sulphate (SDS) 2 h before application of Dfb ointment. This procedure was repeated twice a week for 3 weeks. To confirm the lesional skin condition, transepidermal water loss (TEWL) and scratching behavior were measured before and after each antigen challenge.

2.5. Treatment of AD-like dermatitis

After 3 weeks of Dfb application, mice with scores > 5 were divided into 6 groups. Group 1 mice were untreated, group 2 was treated with vaseline alone (control), group 3 with heparinoid, group 4 with betamethasone, group 5 with tacrolimus, and group 6 with Sema3A ointment, with the latter consisting of 2.5 μg rhSema3A mixed with 1 g vaseline on paraffin film immediately before application. Ointments were applied to the skin once daily for 4 days. TEWL was measured before and after treatment using a Tewameter® TM210 (Courage & Khazawa, Cologne, Germany). On the same days, the mice were videotaped to assess scratching behavior. After treatment, skin samples were collected for immunohistological and histological analyses.

2.6. Clinical skin score

The severity of AD-like dorsal skin lesions was assessed according to four symptoms: erythema/hemorrhage, scarring/dryness, edema and excoriation/erosion. Each symptom was graded from 0 to 3 (none, 0; mild, 1; moderate, 2; severe, 3). Clinical skin score was defined as the sum of the individual scores and ranged from 0 to 12 [11].

2.7. Measurement of scratching behavior

Scratching behavior was observed as described [12]. Mice were placed individually in acrylic cages composed of four cells (13 cm × 9 cm × 35 cm). A camcorder (Model HDR-SR11; Sony, Tokyo, Japan) was positioned above the cages to record the animals' behavior. After an acclimation period of at least 1 h, the animals' behavior was recorded on video for 2 h with no experimenters present in the observation room. Scratching behavior was assessed by replaying each video. Each incidence of scratching behavior was defined as raising to lowering of a leg and changes in number of scratchings from before to after treatment was recorded.

2.8. Immunohistochemistry

Mouse skin was collected from the dorsal neck under sevoflurane anesthesia. Samples were fixed in 4% paraformaldehyde (PFA) in 0.1 M phosphate buffer (pH 7.4) for 4 h at 4 °C. After washing with phosphate-buffered saline (PBS, pH 7.4), small pieces of the skin were immersed successively in PBS containing 10%, 15% and 20% sucrose. These samples were embedded in OCT compound (Sakura Finetechnical) and frozen in liquid nitrogen. Cryosections 8 and 20 μm thick were cut using a CM1850 cryostat (Leica, Wetzlar, Germany) and mounted onto silane-coated glass slides for histological analyses. After blocking in PBS with 5% NDS, 2% BSA and 0.2% Triton X-100, the cryosections were incubated with primary antibodies overnight at 4 °C, washed with PBS containing 0.05% Tween 20 (PBS-T), and incubated with secondary antibodies for 1 h at room temperature. The sections were washed with PBS-T and mounted in Vectashield® Mounting Medium, with immunoreactivity assessed by confocal laser scanning microscopy (DMIRE2; Leica). In control experiments, the primary antibodies were either omitted or replaced by normal IgG.

2.9. Histological analyses

Skin samples were fixed in buffered 20% formalin for 18 h at room temperature and embedded in paraffin. Subsequently, sections 4 μm thick were cut and stained with direct fast scarlet 4BS (DFS), toluidine blue (TB) and hematoxylin–eosin (HE).

2.10. Semiquantitative measurements

The numbers of cutaneous CD4 immunoreactive ($CD4^+$) T cells immunostained with rat monoclonal antibody, mast cells in TB-stained sections and eosinophils in DFS-stained sections were expressed as the means in 3 random fields (1.0×10^5 μm^2) per mouse. Epidermal thickness was measured in 10 random fields (1.0×10^5 μm^2) per mouse. All of these measurements were performed using BZ-H2A software (Keyence, Osaka, Japan). To quantify the number of epidermal nerve fibers, 9 specimens from each mouse were stained with the above-mentioned primary antibodies, and optical sections 0.9 μm thick were scanned through the z-plane of the stained specimens by confocal microscopy. The images were reconstructed in three dimensions using Leica Confocal Software (Leica). For measurements of the numbers of epidermal nerves, we analyzed at least 15 confocal images per group per experiment. The number of epidermal nerve fibers in each 1.6×10^5 μm^2 section of the epidermis was quantified. The number of inflammatory cells and epidermal nerve fibers was counted manually by two researchers (M.T. and K.T.) in a blinded manner. All values represent the means ± SD.

2.11. Statistical analysis

Data were analysed using Prism 5 (GraphPad Software Inc., La Jolla, CA, USA). In all analyses, $P < 0.05$ was regarded as statistically significant.

3. Results

3.1. Induction of AD-like dermatitis

AD-like dermatitis was induced by repeated application of Dfb ointment to the skin of NC/Nga mice for 3 weeks, with Dfb-treated mice showing higher dermatitis scores than controls (Fig. 1A and B). Repeated application of Dfb also increased TEWL (Fig. 1C) and number of scratching behaviors (Fig. 1D).

3.2. Effects of Sema3A ointment on TEWL, dermatitis and scratching behavior

When compared with untreated mice, only the mice treated with Sema3A ointment showed a significant improvement of TEWL (Fig. 2A). Vaseline- and heparinoid-treated mice showed no remarkable changes in TEWL.

Moreover, dermatitis scores were significantly lower in mice treated with Sema3A betamethasone and tacrolimus than in controls (Fig. 2B). No such inhibitory effects were observed in mice treated with vaseline or heparinoid (Fig. 2B).

In addition, the number of scratching behaviors was significantly lower in Sema3A ointment treated than in control mice (Fig. 2C). Although betamethasone and tacrolimus also attenuated the number of scratching behaviors compared with the control group, these effects were not significant (Fig. 2C).

3.3. Effect of Sema3A ointment on epidermal nerve densities

Skin samples from each group were immunostained with anti-PGP9.5 and anti-SP antibodies (Fig. 3A). We found that Sema3A ointment reduced the numbers of both PGP9.5-immunoreactive ($PGP9.5^+$) and SP-immunoreactive (SP^+) fibers in the epidermis of Dfb-treated mice compared with controls (Fig. 3B). The numbers of these nerve fibers were also decreased in betamethasone- and tacrolimus-treated groups, but not in the other groups.

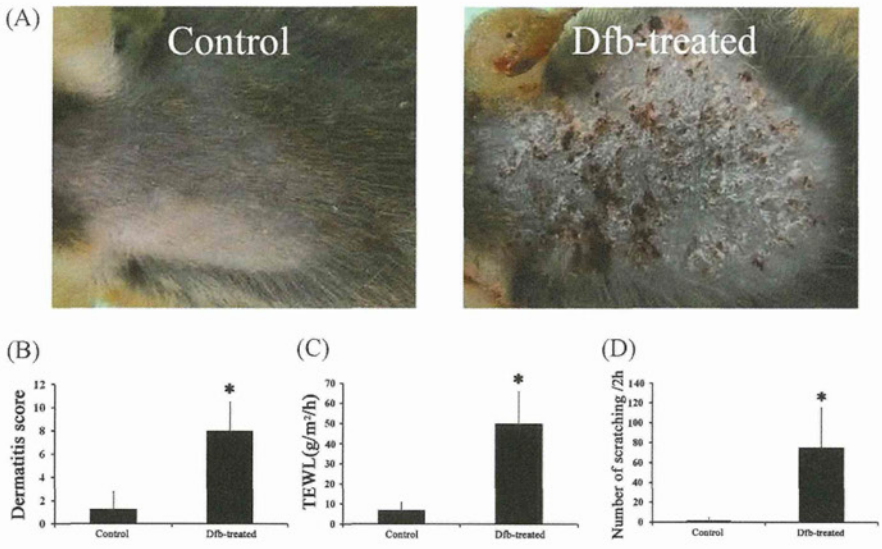

Fig. 1. Repeated application of Dfb induces AD-like symptoms in NC/Nga mice. (A) Following shaving and application of 4% SDS, Dfb (100 mg/site) was applied twice weekly for 3 weeks onto the dorsal skin of NC/Nga mice; control mice were treated with 4% SDS alone. Hemorrhage, scarring, edema and excoriation were observed in Dfb-treated but not in control mice. (B) Dermatitis scores were significantly higher in Dfb than in control mice ($^*P < 0.05$). (C) Transepidermal water loss (TEWL) was greater in Dfb-treated than in control mice ($^*P < 0.05$). (D) Scratching behavior was greater in Dfb-treated than in control mice ($^*P < 0.05$). All results are shown as means ± SD ($n = 5$) and compared by two-tailed unpaired t-tests.